Universidade de Lisboa

Faculdade de Farmácia

INVOLVEMENT OF AQUAPORINS IN HYDROGEN PEROXIDE PERMEATION

Tatiana Viegas Nobre

Dissertação de Mestrado

Mestrado em Ciências Biofarmacêuticas

2015

Universidade de Lisboa

Faculdade de Farmácia

INVOLVEMENT OF AQUAPORINS IN HYDROGEN PEROXIDE PERMEATION

Tatiana Viegas Nobre

Dissertação de Mestrado orientada pela Prof. Doutora Graça Soveral, Faculdade de Farmácia, Universidade de Lisboa

Dissertação de Mestrado coorientada pelo Prof. Doutor Fernando Antunes, Faculdade de Ciências, Universidade de Lisboa

Mestrado em Ciências Biofarmacêuticas

2015

A ti, que foste embora a meio da minha jornada, movido por uma coragem surpreendente...

A ti, que ficaste e foste mais forte, movida por uma força incessante...

Juntos movemos montanhas...Esta vitória é nossa.

Acknowledgments

A realização desta tese de mestrado contou com apoios e incentivos importantes e imprescindíveis sem os quais a sua realização não seria possível. A todos aqueles que de alguma forma, direta ou indiretamente, contribuíram para este meu feito, eu expresso o meu sincero agradecimento:

À Professora Teresa Moura que foi com quem começou todo este meu caminho. Proporcionou-me a entrada no grupo e o conhecimento de pessoas fantásticas. Agradeço-lhe todo o constante acompanhamento e exigência que me permitiram crescer como investigadora e como pessoa.

À Professora Graça Soveral que, como a própria expressou, há alguns anos que estou "debaixo da sua asa" e agora finalizo a minha jornada como estudante com um enorme sentimento de gratidão. Além disso, foi a principal "culpada" da minha candidatura ao mestrado de Ciências Biofarmacêuticas e por essa razão devo-lhe muito do meu crescimento como cientista. Agradeço assim por toda a orientação, motivação, pelas opiniões e críticas, pela oportunidade de ter feito parte do grupo e por toda a confiança depositada.

Ao Professor Fernando Antunes, pela orientação ao longo desta minha etapa, pela partilha de conhecimento, pela disponibilidade e oportunidade de colaboração.

À Doutora Catarina Prista, por me ter acolhido no seu laboratório no Instituto Superior de Agronomia onde iniciei a parte laboratorial da tese e pela orientação, apoio e disponibilidade para tirar todas as minhas dúvidas.

À Ana Paula Martins, pela partilha de conhecimento, disponibilidade, paciência e ajuda nos momentos em mais precisei. À Farzana Sabir pelos ensinamentos e apoio prestado em toda a parte experimental de trabalho realizada no Instituto Superior de Agronomia. À Ana Madeira que sempre esteve disposta a ajudar e a quem devo muito do meu início de jornada no mundo da ciência. E claro à Andreia Mósca e à Cláudia Rodrigues pela disponibilidade constante, conhecimento partilhado, paciência demonstrada perante todas as minhas dúvidas iniciais e pelos bons momentos de pausa e descontração no ISA.

Á Professora Luísa Cyrne, pelo acolhimento no seu laboratório na Faculdade de Ciências da Universidade de Lisboa, e que, apesar de não estar por dentro do meu trabalho, sempre tinha a preocupação de perguntar e querer saber se estava tudo a correr bem. Obrigada pela disponibilidade prestada.

Aos colegas da Faculdade de Ciências da Universidade de Lisboa, Tomás, Carolina e Filipe pelo companheirismo e bons momentos. Um obrigado especial ao Valdir, que me ajudou na integração no laboratório, por todos os seus ensinamentos e paciência demonstrada quando comecei a trabalhar no laboratório.

Aos colegas do mestrado com quem passei bons momentos, e principalmente à Raquel, por estar sempre presente, pela amizade e boa disposição, pelos desabafos e apoio, pelas noitadas a trabalhar e momentos de descontração.

Á minha afilhada académica Lénia pelos momentos partilhados e apoio incondicional à madrinha. Engraçado como parece que às vezes os papéis se invertem.

Aos amigos Mónica, Raquel, Stefanie, Ana Cláudia, Zé, Sérgio e João pelo importante contributo para a minha sanidade mental, pela distração, boa disposição, bons momentos, e amizade que perdura e que não quero perder por nada. Tenho os melhores amigos do mundo.

Ao Telmo com quem tenho partilhado estes últimos quatro anos e a quem tenho que agradecer o companheirismo, apoio incondicional, incentivo, amizade, paciência e a quem tenho que pedir desculpa pelos dias que eu estava chateada, frustrada ou com mau feitio. Tiveste um papel crucial nesta minha etapa e tornaste tudo menos difícil. Obrigada por tudo.

E por último, um agradecimento especial à minha família. Aos meus avós que sempre preocupados demonstram todos os dias o carinho e amor e me tornam mais rica. Também lhes devo muito por tudo isto. Ter uns avós assim vale ouro. Á minha mãe que é um verdadeiro exemplo de coragem e de mulher e que tanto orgulho me dá. Um dia quero ser como tu mãe. Ao meu pai que é o meu herói, das pessoas mais fortes que conheço e que sabe perfeitamente me “passar” um pouco da sua força. Obrigada por teres sempre a palavra certa em momentos complicados da minha vida. Devo a estas duas pessoas o que sou hoje, obrigada por tudo do fundo do coração! Ao meu irmão, que apesar de chato, é o melhor irmão do mundo, e mesmo com a sua tenra idade sabe perfeitamente apoiar e motivar a mana. Obrigado irmão. Estou de coração cheio e amo-vos a todos.

Table of Contents

List of Figures

Figure 3.4. Exemplification of the determination of the rate constants in *S. cerevisiae* strain transformed with empty vector pUG35, i.e. the control cells (A) and *S. cerevisiae* strain transformed with AQP1-isoform (B), AQP3-isoform (C), AQP4-isoform (D), AQP5-isoform (E), AQP7-isoform (F) and AQP11-isoform (G). All the strains were cultured in SC media. In blue is exemplified the typical recording of a H_2O_2 consumption with the H_2O_2 electrode. In grey, it is represented the ln(Voltage) versus time (msec). The rate constant was obtained from the slope of a plot of ln(voltage) versus time.

Figure 3.5. Graphical representation of first-order kinetic rate constant (*k*) of the H_2O_2 consumption obtained for each AQP-transformed strains cultured in SC media, as well as, *k* value obtained by control cells. Data are expressed as mean ± standard deviation (SD). Multiple comparisons test was used to statistical analysis. The comparisons between first-order kinetic rate constant (*k*) of the H_2O_2 consumption obtained by control cells ant the *k* value obtained for each AQP-transformed strains cultured in SC media. Family-wise significance and confidence levels (CI): $P<0.05$ (marked as *) and $P<0.01$ (marked as **) were considered to be statistically significant.

Figure 3.6. Exemplification of the determination of the $k_{catalase}$ in *S. cerevisiae* permeabilized cells transformed with empty vector pUG35, i.e. the control permeabilized cells (A) and *S. cerevisiae* permeabilized cells transformed with AQP3-isoform (B), AQP4-isoform (C) and AQP5-isoform (D). In blue are exemplified the typical recording of a H_2O_2 consumption by catalase. In orange it is represented the plot of ln(voltage) versus time (msec). The rate constant was obtained from the slope of a plot of ln(voltage) versus time.

Figure 4.1. Correlation between the fluorescence signal intensity quantified and the rate constant (*k*) calculated for the consumption of H_2O_2 for each AQP-isoform expressed in *S. cerevisiae* strains cultured in SC media. In blue are represented the *k* values (in sec^{-1}) obtained for each AQP-isoform, with H_2O_2 free diffusion deducted (*k* value calculated for control strain). The yellow bars identify the fluorescence intensity of signal, classifying the AQP-expression level.

Figure 4.2. Normalized H_2O_2 consumption for each AQP-expressing strains. The normalization was achieved by using the equation: $[(consumption_{AQP} - consumption_{control})/expression\ level]$.

List of Tables

Resumo

As aquaporinas (AQPs) são uma família de proteínas transmembranares que desempenham um papel crucial a nível fisiológico e patológico na célula, em particular na progressão de alguns tipos de cancro. O seu envolvimento em várias patologias, tal como no cancro, pode ser devido à sua disfunção como canal celular, ou devido ao efeito das moléculas transportadas. Um exemplo é a molécula de H_2O_2, que está envolvida em processos celulares associados a condições de saúde e doença, e foi recentemente identificado o seu transporte pela AQP3. O conhecimento da regulação das AQPs, bem como da sua capacidade de permear moléculas que são intervenientes em vias de sinalização celular, como o H_2O_2 que está diretamente associado ao stresse oxidativo, seria um ponto de partida na identificação de novos alvos para abordagens terapêuticas. Tendo em conta o envolvimento de H_2O_2 em várias condições patológicas, e o facto de esta molécula estar associada com a progressão tumoral, este projeto visa investigar o papel das AQPs na permeação do H_2O_2. Para isso, um sistema de expressão heteróloga em *Saccharomyces cerevisiae* foi utilizado com o intuito de estudar o papel de algumas isoformas de AQP de mamífero na permeação de H_2O_2. Numa primeira análise, foi investigado o crescimento das diferentes estirpes na presença de diferentes concentrações de H_2O_2 através de um ensaio fenotípico. Posteriormente, o consumo de H_2O_2 das diferentes estirpes foi medido utilizando um elétrodo de H_2O_2, e os parâmetros cinéticos foram determinados para avaliar o transporte de H_2O_2 através das diferentes isoformas de AQPs de mamífero. Foram determinados os respetivos níveis de expressão na membrana plasmática das seis isoformas de AQPs de mamífero estudadas, valores estes utilizados para a normalização das constantes de velocidade obtidas do consumo de H_2O_2. Em comparação com as células de controlo que expressam o plasmídeo vazio, as estirpes que expressam as isoformas AQP3, AQP4 e AQP5 revelaram uma taxa de permeação elevada (cerca de 40%, 50% e 60% respetivamente). Além disso, nestas estirpes transformadas a atividade da catalase, uma enzima antioxidante responsável pela degradação da molécula de H_2O_2, não é superior à atividade determinada nas células de controlo, confirmando-se assim que o metabolismo associado à degradação de H_2O_2 não está aumentado nas estirpes transformadas. Concluindo, os nossos resultados sugerem que, entre todas as isoformas de AQP testadas, a AQP3 e AQP4 facilitam a difusão de H_2O_2, e que a AQP5 mostra uma permeabilidade significativamente superior às outras isoformas. Estes dados apontam para o papel fisiopatológico da AQP5 que pode estar relacionado com a sua capacidade de transportar H_2O_2 que é uma molécula interveniente no stress oxidativo.

Abstract

Aquaporins (AQPs) are a family of transmembrane proteins that have been revealed as having an important role in cell physiology and pathology, in particular in the progression of some types of cancer. The involvement of AQPs in several pathologies, such as in cancer, may be due to their dysfunction as channels and/or due to the effect of their transported molecules. An example is H_2O_2, a molecule involved in cellular processes associated with health and disease conditions and recently identified as transported by AQP3. Therefore, the knowledge of AQPs regulation, as well as their ability to permeate molecules involved in signaling pathways in cell, such as oxidative stress triggered by H_2O_2, would enable to identify novel targets for therapeutic approaches. Due to the evidences on H_2O_2 involvement in several pathological conditions, and their association with tumor progression, this project aims to investigate the role of AQPs in H_2O_2 permeation. For this purpose, yeast *Saccharomyces cerevisiae* strains genetically modified to express individual mammalian AQPs were used to assess the permeability of H_2O_2. In a first approach, the growth of each AQP-transformed strain was analyzed in presence of different H_2O_2 concentrations in a phenotypic assay. Then, the H_2O_2 consumption of each AQP-transformed strain was measured using a H_2O_2 electrode, and the kinetic parameters were determined for the assessment of membrane H_2O_2 permeation through the different mammalian-AQPs. For the six mammalian-AQPs analyzed, their level of expression at the plasma membrane was measured and used to normalize the rate constant of H_2O_2 consumption. Compared to control cells expressing the empty plasmid, AQP3-, AQP4- and AQP5-expressing strains showed a higher permeation rate (about 40%, 50% and 60% respectively). In addition, in these strains the catalase activity, an antioxidant enzyme responsible by H_2O_2 degradation, was not higher than control, assuring that H_2O_2 metabolism is not altered. In conclusion, our results show that among all the tested aquaporins, AQP3, AQP4 and AQP5 permeate H_2O_2, and that AQP5 shows a significantly higher permeability than the other isoforms. These data suggest that the mechanism of AQP5 involvement in physiopathology may be related to its capacity to transport H_2O_2 and interference in oxidative stress.

Keywords: Aquaporins; permeability; hydrogen peroxide; yeast; heterologous expression, catalase.

Abbreviations and Symbols

AKT	Protein kinase B
AQP(s)	Aquaporin(s)
ATP	Adenosine triphosphate
E_a	Activation energy
EGF	Epidermal Growth Factor
ESCC	Esophageal squamaous cell carcinoma
GFP	Green Fluorescence Protein
GPx	Glutathione Peroxidase
GSH	Glutathione
H_2O_2	Hydrogen Peroxide
k	First-order kinetic rate constant
$k_{catalase}$	Rate constant of catalase activity
MAP (kinase)	Mitogen-activated protein kinase
NADPH	Nicotinamide adenine dinucleotide phosphate
Nox	NADPH Oxidases
OD	Optical Density
pA	Picoampere (1pA = 10^{-12}A)
P_f	Osmotic water coefficient
PTEN	Phosphatase and tensin homolog
Prx	Peroxiredoxins
rASMCS	Rat aortic smooth muscle cells
ROS	Reactive Oxygen Species
S. Cerevisiae	*Saccharomyces cerevisiae*
SC (media)	Synthetic complete media
shRNA	Small hairpin RNA
siRNA	Small interfering RNA
V_w	Water molar volume (18 cm^3 mol^{-1})
YNB	Yeast Nitrogen Base
ε	Molar extinction coefficient = 43.4 $M^{-1}cm^{-1}$

1. Introduction

1.1 AQUAPORINS

Water is the most abundant molecule in organisms constituting more than half of and individual body weight. Water is present in all cells and tissues in and out of the cell compartments, and is indispensable for life. Due to the high water permeability of the plasma membrane, cells are usually very sensitive to osmotic gradients that are able to cause volume changes. This fact may result in several problems, especially in cells entrapped in rigid or inextensible compartments (e.g. central nervous system), which requires the existence of regulatory mechanisms (Moura, 2004). The transmembrane proteins channels aquaporins (AQPs) are a family of integral membrane proteins, whose primary function is water and/or glycerol transport (Maeda, Funahashi, & Shimomura, 2008; Moura, 2004). For this reason, AQPs play a crucial role in the regulation and maintenance of homeostasis.

1.1.1 The discovery of Aquaporins

For decades, the simple diffusion model explained the water flow through the phospholipid bilayer. However, in the fifties, the existence of water channels was hypothesized by Solomon and co-worker (Sidel & Solomon, 1957) to explain the high membrane water permeability observed in red blood cells that could not be justified by a simple diffusion process (Benga, 2003). In 1970, Macey described the inhibitory effect of mercurial compounds (such as mercury chloride). They demonstrated a reversible variation of plasma membrane water permeability and subsequent increase of activation energy in response to the application of this type of blocking agents (Macey & Farmer, 1970).

The disclosure of AQPs as a specific transport water channel was reported by Peter Agre and co-workers in 1987. This membrane protein was accidently isolated and purified with the Rh blood group antigen from cell membranes of erythrocytes (Agre, Saboori, Asimos, & Smith, 1987). Afterwards, this contaminant protein with 28 kDa was designated as CHIP28 "*channel-like integral protein of 28 kDa*" (Smith & Agre, 1991). Also in 1991, the protein sequence was discovered (Preston & Agre, 1991) and showed homology to other uncharacterized protein MIP26 (*26- kDa Major Intrinsic Protein*) from bovine lens cells, already described by Gorin (Gorin, Yancey, Cline, Revel, & Horwitz, 1984). These data suggested that CHIP28 belongs to the transmembrane protein channels MIP family(*Major Intrinsic Protein*) (Smith & Agre, 1991). Experiments performed in 1992, as the heterologous expression of CHIP28 in *Xenopus* oocytes (Preston, Carroll, Guggino, & Agre, 1992) and the CHIP28 insertion in liposomes (Zeidel, Ambudkar, Smith, & Agre, 1992), revealed important evidences of water channel activity by CHIP28. In 1993, the CHIP28 was renamed as aquaporin-1, as it is known nowadays. In 1999

Peter Agre reported the first high-resolution image of AQP1 three-dimensional structure (Mitsuoka et al., 1999). A few years later, all the work developed by Agre and co-workers in the discovery and characterization of AQP1 was recognized as the Nobel Prize in Chemistry 2003.

1.1.2 Structure of Aquaporins

From the structural point of view, AQPs exist in membrane as tetramers, as shown in figure 1.1, and each monomer is a specific channel for water and/or other solutes, like glycerol. The tetrameric assembly seems to be crucial for the correct folding, stability, targeting to the plasma membrane and even functionality of AQPs (Hachez & Chaumont, 2010).

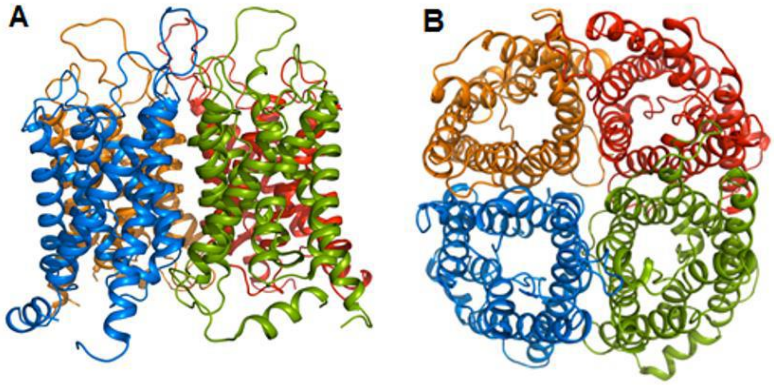

Figure 1.1. In A (lateral view) and B (top view), this represented the tetramer AQP1 where each color corresponds to a different monomer. Adapted from (Soveral 2011).

In figure 1.2, the structure of one monomer is represented and the pore structure and its organization can be viewed: six transmembrane helices with NH_2- and COOH-termini located on the cytoplasmic side, linked by 5 loops. The loops B and E contain two short hydrophobic stretches of amino acid residues asparagine-proline-alanine (NPA), highly conserved and considered as the signature sequences for AQPs (Ishibashi, Kondo, Hara, & Morishita, 2011; Moura, 2004). These two NPA motifs act as selectivity filters for water permeation. However, the AQP selectivity results from the combination of two selectivity filters, the NPA motifs and the aromatic/arginine filter (ar/R), the narrowest region of the pore. The presence of these particular hydrophilic and hydrophobic residues makes the AQP pore able to exclude molecules due the charge characteristics or molecular size. In other words, the selectivity filters confer the capacity to avoid permeation to protons or any solutes above 2.8 Å in human AQP1 (the diameter of a water molecule), and above 3.4 Å for the less selective aquaglyceroporins (Almasalmeh, Krenc, Wu, & Beitz, 2014; Verkman, Anderson, & Papadopoulos, 2014).

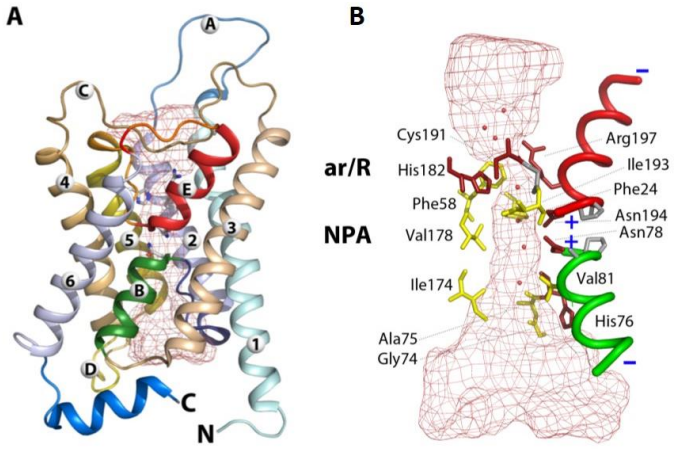

Figure 1.2. In A, is shown the structure of a monomer of AQP1 of ox, with six helices numbered 1 to 6, and the loops identified with letters A through E. In B, are represented the half helices (in red and green) and the hydrophilic and hydrophobic residues (in red and yellow, respectively), which constitute the pore. The selective filters (ar/R and NPA motif) are also shown. Adapted from (Soveral 2011).

1.1.3 Selectivity of Aquaporins

Aquaporins can be divided into orthodox or classical aquaporins (selective for water) and aquaglyceroporins which in addition to water, transport small solutes including glycerol. There are 13 AQPs identified in mammalians (AQP0-12) with a similar structure and differing only in some amino acids located in crucial points which confer to the two subfamilies (orthodox and aquaglyceroporins) the ability of glycerol permeation as well as other solutes. The initial ten members of the mammalian AQPs (AQP0-9) are relatively well described, while the characterization and functions of the three last identified members AQP10, AQP11 and AQP12 are not completely known. The AQP11 and AQP12 were considered as members of a new subfamily (Superaquaporins), and there are evidences about their sub-cellular localization in different cell types; however, these data are controversial (Ishibashi, 2009). The aquaglyceroporins AQP3, AQP7, AQP9 and AQP10 represent a subfamily that allows movement of water (typically low water permeability) and other small solutes, such as glycerol, urea, reactive oxygen species (hydrogen peroxide) and gases (ammonia, carbon dioxide and nitric oxide) and even some ions (Almasalmeh et al., 2014; Verkman et al., 2014). However, the physiological role of some aquaglyceroporins is not fully understood. Recently, it was reported that AQP3 and AQP8 can promote the H_2O_2 uptake into mammalian cells, while the orthodox aquaporin (AQP1) cannot facilitate the membrane H_2O_2 permeability (Bienert et al., 2007; Miller, Dickinson, & Chang, 2010). Table 1.1 summarizes the functional characterization of each AQP, as well as its tissue distribution.

Table 2.1. Permeability characteristics and tissue distribution of mammalian aquaporins.

Aquaporin	Permeability	Tissue Distribution
AQP0	Water (low)	Lens epithelium (Day et al., 2014)
AQP1	Water, CO_2, NO (Carbrey & Agre, 2009)	Kidney, skin, blood vessels, liver, pancreas, lung, eye, brain (Day et al., 2014)
AQP2	Water	Kidney collecting duct cells (Day et al., 2014)
AQP3	Water, glycerol, H_2O_2 (Miller et al., 2010)	Kidney, skin, lung, eye, colon, stomach (Day et al., 2014)
AQP4	Water	Astrocytes, skeletal muscle, kidney, lung, inner ear, colon, small intestine, stomach, retina, olfactory epithelium, spinal cord (Day et al., 2014)
AQP5	Water	Salivary, lacrimal and sweat gland, lung, cornea, trachea, stomach (Day et al., 2014)
AQP6	Water (low), anions (NO^-_3) (Carbrey & Agre, 2009)	Kidney (Day et al., 2014)
AQP7	Water, glycerol, urea (Carbrey & Agre, 2009), arsenite (Z. Liu et al., 2002)	Adipose tissue, kidney, testis, ovaries (Day et al., 2014)
AQP8	Water, urea, ammonia (Carbrey & Agre, 2009), H_2O_2 (Bienert et al., 2007)	Testis, kidney, liver, pancreas, small intestine, colon, spinal cord, ovaries (Day et al., 2014)
AQP9	Water (low), glycerol, urea (Carbrey & Agre, 2009), arsenite (Z. Liu et al., 2002)	Liver, leukocytes, brain, testis, small intestine, ovaries (Day et al., 2014)
AQP10	Water (low), glycerol, urea (Carbrey & Agre, 2009)	Skin, Small intestine (Ishibashi, 2009)
AQP11	Water, glycerol (Madeira et al., 2014)	Brain, testis, liver, kidney (Ishibashi, 2009), adipocytes (Madeira et al., 2014)
AQP12	Not known	Pancreas (Ishibashi, 2009)

1.1.4 Biological Function and Associated Diseases

As mentioned above, AQPs are involved in the transport of water but also in the permeation of small solutes such as glycerol, hydrogen peroxide (H_2O_2), in some cases urea or even gases. Several functions such as cell volume regulation, energy metabolism, cell migration, adhesion, proliferation and differentiation are regulated by AQPs, and therefore they play an important role in physiological actions such as osmoregulation, lipid metabolism, organogenesis and regenerations, and vascular and cancer biology (Ishibashi et al., 2011; Verkman, 2011).

The different AQPs tissue distribution originates a diversity of AQP functions, and naturally its disruption can lead to different phenotypes or pathologies (known as aquaporinpathies). Knock-out mice have been helpful in the discovery of the physiological significance of AQPs (Ishibashi et al., 2011; Verkman, 2009). It was identified that AQP0 is involved in maintaining lens transparency, and its disruption can produce cataracts (Carbrey & Agre, 2009). On the other hand AQP7 is highly expressed in adipose tissue and, together with AQP9 that is expressed in

the liver, are key metabolic regulators in obesity and possibility in diabetes. AQP4 is mainly expressed in brain cells (e.g. astrocytes but not neurons) and is associated to brain swelling. AQP3 play a crucial role in keeping skin moisture and additionally has an important role in skin regeneration and skin tumor progression (Ishibashi, Hara, & Kondo, 2009; Ishibashi et al., 2011; Verkman, 2009, 2011). Therefore, modulation of AQPs expression/function might be a novel target for clinical benefit in treatment of numerous diseases, such as obesity, epilepsy, glaucoma, brain edema, and cancer.

1.1.4.1 Role of Aquaporins in Cancer

Previous studies reported overexpression of several AQPs in some types of tumors and that these membrane proteins facilitate cell migration and proliferation (Verkman, 2009). In several tumors it is supposed to exist a relationship between histological tumor grade and the level of AQP expression (Verkman, Hara-Chikuma, & Papadopoulos, 2008). AQP1, AQP4 and AQP5, are strongly expressed in brain tumors, and additionally AQP1 is broadly expressed in other cancer tissues like lung, prostate, ovary, colon, colorectal and mammary carcinoma (Nico & Ribatti, 2010). An experimental model using AQP1 knockout mice reported an association between AQP1 and tumor progression, including cell migration and angiogenesis. Interestingly, AQP1 is highly expressed in proliferating tumor microvessels, which supports the AQP1 association with angiogenesis (Nico & Ribatti, 2010). Overall, it is speculated that AQPs overexpression in tumor cells is correlated with the permission of rapidly water entrance into growing tumor mass, leading to tumor expansion, as reported in tumor-associated edema and in brain tumors.

Several studies described that AQP5 has a crucial role in the development of several cancer types and report an increase in AQP5 expression in pancreatic, colon, colorectal, lung, human ovarian, myelogenous leukemia and, more recently in human breast cancer cells (Chae et al., 2008; Machida et al., 2011; Shi et al., 2012; Woo et al., 2008; Yang, Yan, Zheng, & Chen, 2012; Zhang et al., 2010). It has been demonstrated that AQP5 expression is associated with induction of cell proliferation and metastasis of cancer cells. Besides, this AQP-isoform was described as able to promote inhibition of apoptosis, and thereby high expression levels of AQP5 can be associated with resistance to cancer treatment (Nico & Ribatti, 2010; Shi et al., 2012). For that reason, AQP5 can also be a critical target for oncotherapy. In fact, AQP5 was already reported as a novel biomarker for colorectal cancer aggressiveness and metastasis (Shan, Cui, Li, Lin, & Li, 2014), as well as for prostate cancer (Li et al., 2014). Recently, a study discovered that both AQP3 and AQP5 expression levels in esophageal squamaous cell carcinoma (ESCC) tissues were

significantly increased and correlated with advanced invasion depth, aggressive lymph node status and distant metastasis, but interestingly, the overexpression of AQP3 and AQP5 alone did not influence the prognosis. Thus, it is postulated that the combined detection of two AQP-isoforms can be beneficial to predict the progression, as well as the prognosis of ESCC patients (S. Liu, Zhang, Jiang, Yang, & Jiang, 2013).

While previous studies referred that some AQPs are overexpressed in several types of cancer cells, other studies reported that in several cancers there is reduction of expression of a given AQP. For example, in human colorectal cancer, there is overexpression of AQP1, AQP3 and AQP5, but there is reduction of AQP8 expression (Verkman, 2008). It has been demonstrated that expression of AQP8 and AQP9 is highly decreased in hepatocellular carcinoma. The authors suggest that this AQP deficit can be due to an increased resistance to apoptosis for this type of cancer, because apoptosis is characterized by reduced cell size due to changes in intracellular ion concentration and rapid AQP-dependent water efflux (Jablonski et al., 2007).

Aquaglyceroporin-3 expression was demonstrated in some tumor tissues like colorectal carcinoma and kidney collecting duct carcinoma (Kafe, Verbavatz, Cochand-Priollet, Castagnet, & Vieillefond, 2004; Moon et al., 2003). In addition, AQP3 was detected in lung carcinomas and adenocarcinomas. Liu et al. reported that lung carcinomas and adenocarcinomas are able to produce AQP3 within their functional and/or biological nature. Although the correlation and/or influence of AQP3 in neoplastic lung tissues is not fully known, these data suggest an important role of AQP3 in neoplastic lung cells (Y. L. Liu et al., 2007). Moreover AQP3 is considered to be responsible for keeping skin moisture and proposed to de important in skin regeneration and tumor progression (Nico & Ribatti, 2010; Verkman, 2011). It has been demonstrated that AQP3 is overexpressed in skin carcinomas and in 2008 an experimental study using AQP3 null mice showed an increased resistance to skin tumor formation, among other evidences such as dry skin, impaired cell proliferation and altered fat metabolism (Nico & Ribatti, 2010; Verkman et al., 2008). The observed phenotypes and evidences were caused by absence of glycerol in internal stratum corneum and epidermal cells, i.e. due absence of AQP3 for to transport glycerol into the cells (Verkman et al., 2008) and a mechanism in which the glycerol is a key regulator of ATP production in epidermal cells was suggested. In this case, a reduction of the intracellular concentration of glycerol would consequently decrease the formation of G3P (glycerol-3-phosphate) by glycerol kinase, which is as a key metabolic intermediate in ATP synthesis. A deficit of ATP would trigger a decrease of ATP-facilitated MAP kinase signaling and therefore prevent the activation of the MAP kinase proteins mechanism that stimulates the proliferation of cancer cells. This mechanism also suggests the contribution of glycerol to lipid synthesis, and a capacity of tumor cells for a positive feedback in order to increase cell proliferation (Nico &

Ribatti, 2010; Verkman, 2008; Verkman et al., 2008). Overall, tumor cells have a characteristic strong energy metabolic profile that turns these cells able to compete with surrounding cells and proliferate. However, despite glycerol may be seen as an essential source for tumor progression, further studies are necessary to explain its involvement in tumor progression. On the other hand, there is the possibility that the progression of tumors with AQP3-overexpressed can be due not only to glycerol but to others AQP3-transported solutes as well. As mentioned above, AQP3 is involved in the transport of hydrogen peroxide (H_2O_2), the most abundant reactive oxygen specie (ROS) in the organism (Folmer et al., 2008), which has for long been correlated with tumor development (Fruehauf & Meyskens, 2007).

1.1.5 Functional Studies of Aquaporin Activity

The functional studies of AQPs are performed through water and solutes transport assays. Water moves from one cellular compartment with lower osmotic pressure to another compartment with higher osmotic pressure. Thus, when there is a perturbation in a cellular system, an osmotic gradient is generated, and the water moves to establish an osmotic equilibrium. In order to assess the AQP activity, the osmotic water coefficient (P_f) can be measured in cells subjected to osmotic perturbation at different temperatures, as well as the activation energy of water transport (E_a). Due to the relationship between the rate of cell volume change and the cell membrane permeability, the changes of cellular volume can be measured along the time of osmotic shock. The stopped flow technique is a useful method to detect rapid volume changes of cells by rapid mixing with hypo- or hyperosmotic solutions inducing cells to swell or to shrink until they reach a new equilibrium volume. A method to detect volume changes is by loading cells with a volume sensitive fluorescent probe. Thus, cells are osmotically challenged in the stopped flow device, and cell swelling or shrinkage in followed by the consequent change in the fluorescence signal output. Afterwards, the fluorescent signals are fitted to an exponential function and the water permeability is calculated, through the equation: $P_f = k\ (V_0 / A)[1 / V_w\ (osm_{out})_\infty]$, where k is the rate constant, V_0 is the initial volume before the osmotic shock, V_w is the water molar volume (18 $cm^3\ mol^{-1}$), $(osm_{out})_\infty$ is the final medium osmolality and A is the cellular area. By experimentally evaluating Pf along a temperature range, the activation energy E_a of transport can be evaluated by the slope of an Arrhenius plot (ln P_f as a function of 1/T, where T is the absolute temperature). Thus, the assessment of AQPs function and its regulation by specific modulators can be characterized using this methodology (Soveral, 2011).

It is worth mentioning that cells frequently express more that one aquaporin isoform in the plasma membrane and that unless a specific isoform is mutated or overexpressed, its function is not easily discriminated. Thus, to individually characterize the selectivity of a given aquaporin, a cell model possessing only one aquaporin isoform is desirable. In this work, the yeast heterologous expression system was used to assess aquaporin permeation to H_2O_2.

The yeast model in a proven model eukaryote for several studies of basic cellular and molecular processes, and has been gained special interests for studies that target disease-associated molecular events, as well as to the finding of novel medicinal compounds. Nowadays, the yeast genome is well defined and is easy to manipulate through modifications, such as gene deletion, gene overexpressing and mutations. Moreover, there are yeast mutant collections available commercially. These advantageous features and the fact that the yeast model allows the establishment of similar regulatory and functional conditions to mammalian cells, this model is considered the most attractive tool in cellular and molecular studies for medical and therapeutic research (Mager & Winderickx, 2005).

The yeast heterologous expression system is a widely used approach to study and characterize the activity of AQPs. *Y*east cells, such as *S. cerevisiae*, in particular strains genetically manipulated with deletion of endogenous aquaporins (AQY1 and AQY2 knock-out) can be transformed for heterologous expression of mammalian AQPs, enabling to assess individual activity of aquaporin isoforms.

1.2 HYDROGEN PEROXIDE, A REACTIVE OXYGEN SPECIE (ROS)

In biological systems, H_2O_2 is known as a reactive oxygen specie (ROS), which are species highly cytotoxic. The H_2O_2 molecule has mild reactivity, but in the presence of transition metals, such as iron, it is a precursor of the very toxic hydroxyl radical. In contrast, in low concentrations, H_2O_2 has been identified as having an indispensable role in some important biological process associated to cell function and survival. Thereby, the concentration of this reactive specie needs to be controlled to maintain the cellular homeostasis (Bienert, Schjoerring, & Jahn, 2006). H_2O_2 is produced in various metabolic processes of cells in aerobic organisms, like mitochondrial oxygen metabolism in electron transport chain, or can be formed by enzymes responsible for ROS production, like NADPH oxidases (Nox), xanthine oxidase, and other oxidases (Folmer et al., 2008; Fruehauf & Meyskens, 2007; Wittmann et al., 2012).

1.2.1 Reactive Oxygen Species - health and disease conditions

Due the reactive nature of ROS, they can damage proteins, lipids or nucleic acids. For this reason, in normal conditions there are scavenging systems, like antioxidant enzymes, which catalyze or reduce reactive molecules in order to maintain the low and constant ROS concentration, and to avoid the consequences of ROS accumulation in the cell (Bienert et al., 2007; Fruehauf & Meyskens, 2007; Wittmann et al., 2012). Nevertheless, in abnormal conditions when there is a disruption of the regulation of redox balance, ROS can initiate several signal pathways leading to oxidative stress and/or disorders. Thus, ROS are emerging as critical signaling molecules (Fruehauf & Meyskens, 2007), because they play important roles in cellular processes associated with health and disease conditions. Firstly, it was only known the role of H_2O_2 like an oxidative stress interferer, which can cause oxidative damage to cellular protein, nucleic acids or others molecules. Nowadays it is known that ROS, including H_2O_2, are involved in essential functions in physiological signaling pathways, like differentiation and growing, migration and immune system function (Hara-Chikuma et al., 2012; Lippert et al., 2011).

Currently, there are evidences about association of ROS with several pathological conditions including age-related diseases stages: neurodegeneration (Lin & Beal, 2006), diabetes (Pop-Busui, Sima, & Stevens, 2006) and cancer (Fruehauf & Meyskens, 2007; Lippert et al., 2011). The ROS play a role in carcinogenesis initiation because they react with nucleic acids or chromatin protein resulting in base modifications, genomic instability and alterations in expression of genes. Moreover, it has been reported that ROS are molecules involved in important cellular pathways associated to cancer development as cellular proliferation, apoptosis suppression and angiogenesis. For example, ROS are able to inactivate the protein

PTEN (Phosphatase and tensin homolog) or others phosphatases, that are proteins involved in inhibition of serine/threonine kinase AKT/protein kinase B phosphorylation, a crucial step in cell signaling of growth factors, including cell survival, angiogenesis and migration (Fruehauf & Meyskens, 2007; Fruehauf & Trapp, 2008; Manning & Cantley, 2007). The ROS-mediated DNA damage, with oncogene overexpression, and ROS-mediated signaling, with inhibition of protein phosphatases, contribute both to cellular proliferation and apoptosis suppression. Furthermore, the increasing number of malignant cells leads to a hypoxic environmental that activates angiogenesis (Fruehauf & Meyskens, 2007). Figure 1.3 shows the tree stage processes of cancer development, initiation, promotion and progression, and their relation with the level of ROS or oxidative stress.

It was recently revealed by studies in cancer biology, the role of ROS in melanoma. This involvement of ROS was referred by Fruehauf et al. as “an Achilles’ heel of melanoma”, once melanoma is unique among tumors able to generate ROS in high levels, which can lead to abnormal proliferation, apoptosis suppression, chemotherapy resistance and angiogenesis promotion. In melanoma there are structurally aberrant melanosomes, which under normal conditions are responsible for the protection of cell by scavenging of ROS generated by sunlight and by cellular metabolism; but in pathological conditions, they are able to produce free radicals (Fruehauf & Trapp, 2008).

For these reasons, ROS, such as H_2O_2, their involvement in cancer biology and the study of ROS-modulators have gained specially attention for cancer therapy research, particularly for melanoma treatments due to excess of ROS produced by aberrant melanosomes.

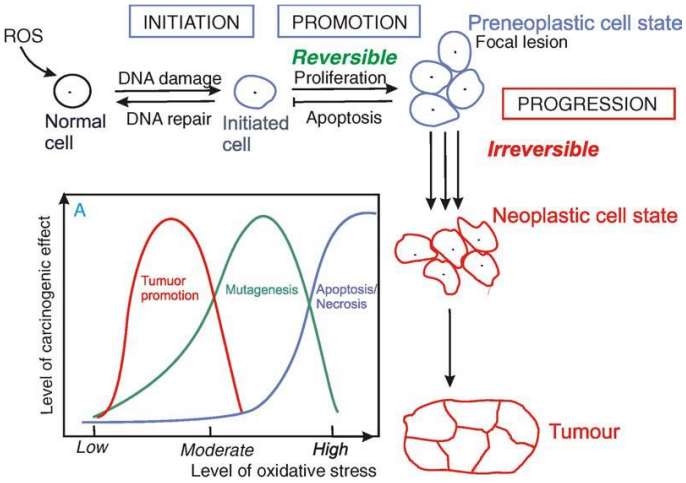

Figure 1.3. Three stages model of carcinogenesis and relation with level of oxidative stress triggered by ROS. Adapted from (Valko, Rhodes, Moncol, Izakovic, & Mazur, 2006).

1.2.2 H_2O_2 permeation by Aquaporins

H_2O_2 is continuously produced intracellularly as a product of cellular metabolism, but can be also generated in extracellular side of cell membranes by Nox proteins. Due this natural extracellular H_2O_2 generation, the investigation of how cells seize H_2O_2 toward beneficial pathways have gained especial interested. H_2O_2 has long been thought to diffuse freely across membranes. However, some membrane systems impose a permeability barrier to H_2O_2 diffusion (Antunes & Cadenas, 2000). These evidences suggested the presence of H_2O_2 uptake regulators, probably membrane proteins, such as channel proteins. In order to discover the H_2O_2 diffusion-facilitating channel proteins, some research groups investigated the H_2O_2 transport across membrane.

Some features like size and electro-chemical properties of solutes were crucial determinants to the transport by AQPs. Interestingly, there are several physico-chemical similarities between hydrogen peroxide and water molecules. In addition, both are able to form hydrogen bonds, which are crucial to permeate the pore, and the H_2O_2 molecule has a diameter of about 0.25-0.28 nm, which is lesser than the pore diameter of AQP1, a typical orthodox-aquaporin (Bienert et al., 2006). These similarities evidence and reinforce the possibility of certain AQPs having the capacity and selectivity to transport these to molecules.

Henzler and co-workers showed the first experimental evidences using a well-studied model system for plants, the internodal cells of the algae *Chara corallina* (Henzler & Steudle, 2000). They simulated the H_2O_2 transport across membranes and estimated transport parameters. After testing the model, they obtained a H_2O_2 permeability coefficient very close to water permeability. Furthermore, they implemented the control test with mercuric chloride. Mercurial compounds were the first blockers of AQPs referred in the literature, however these reagents exhibit high toxicity, and therefore they have not any therapeutic role. In brief, the simple interpretation of their mechanism of action consists in a reaction with sulfhydryl groups in AQPs resulting in covalent modifications, conformational changes and a closure of water channels (Haddoub, Rutzler, Robin, & Flitsch, 2009). After the experiment with the mercurial compound, Henzler and co-workers observed that H_2O_2 permeability was substantially reduced, which indicated that H_2O_2 permeates through AQPs (Bienert et al., 2006; Henzler & Steudle, 2000).

Currently, specific mammalian AQP-isoforms have been identified as candidates for the transport of H_2O_2 across plasma membranes (Bertolotti et al., 2013; Bienert & Chaumont, 2014; Bienert et al., 2007; Dynowski, Schaaf, Loque, Moran, & Ludewig, 2008; Hara-Chikuma et al., 2012).

A recent study demonstrated that the aquaglyceroporin-3 (AQP3) and the non-orthodox aquaporin-8 (AQP8) could promote the H_2O_2 transport across cell membrane in mammalian cells (Bienert et al., 2007; Miller et al., 2010). Using the genetically encoded fluorescent H_2O_2 sensor, Hyper, which detects low levels of H_2O_2, they demonstrated that permeation of H_2O_2 is mediated by AQP3, and these transmembrane proteins can increase or reduce downstream signaling pathways dependent of H_2O_2. They used a human colon cancer adenocarcinoma cell line, which naturally express AQP3 and Nox proteins, in order to assess the association between H_2O_2 production by Nox and the H_2O_2 transport by AQP3 and their influence in downstream signaling cascades H_2O_2 dependent, such as AKT signaling. Moreover, they studied the stimulation of epidermal growth factor (EGF) signaling in the presence of a Nox inhibitor DPI (diphenyleneiodonium), a shRNA against AQP3 and an antioxidant enzyme, catalase. EGF stimulation can activate a Nox protein and consequence extracellular H_2O_2 production, which can pass into the cell through AQP3. The DPI, as a general Nox inhibitor, avoided the extracellular H_2O_2 production; the shRNA was used for the silencing of AQP3 expression, and extracellular catalase was used to destroy extracellular H_2O_2. Figure 1.4 shows a schematic representation of H_2O_2 production by Nox proteins, and its AQP3-mediated transport, as well as the modulators used by Miler et al. in the experimentations. As expected, it was observed a similar effect in the EGF signaling decrease by DPI, extracellular catalase and shRNA against AQP3. The authors established that AQP3 can modulate intracellular redox signaling, including cellular pathways associated with cell growth, proliferation and survival (Miller et al. 2010). These evidences also support that AQP3 can mediate the accumulation of H_2O_2 into mammalian cells, which in turn is associated with progression of tumors, like melanoma.

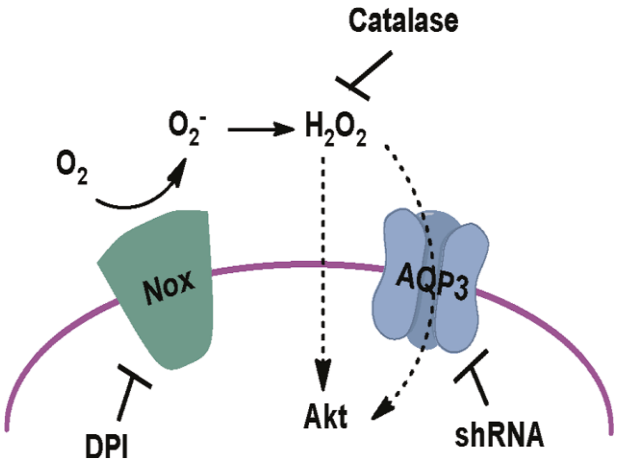

Figure 1.4. Schematic illustrating where the H_2O_2 redox signaling can by intercepted using the DPI, catalase and shRNA modulators. Adapted from (Lippert, Van de Bittner, & Chang, 2011)

Another study performed by Hara-Chikuma and co-workers (Hara-Chikuma et al., 2012) provided evidence concerning to AQP3 role in H_2O_2 permeation in chemokine-dependent T lymphocyte migration during the immune response. They observed that AQP3 is expressed in $CD4^+$ T cells and their trafficking during cutaneous immune reactions was dependent on AQP3-mediated H_2O_2 uptake, but not AQP3-mediated water/glycerol transport. It was also reported that the extracellular H_2O_2 probably produced by Nox NADPH oxidases was transported by AQP3, and is involved in activation of Cdc42 (a Rho family small GTPase) and consequent reorganization of T cells actin cytoskeleton, resulting in a T cell trafficking in response to chemotactic signals. The authors showed that during the cutaneous immune reaction, the trafficking of T cells was impaired in AQP3 knockout mice (Bienert & Chaumont, 2014; Hara-Chikuma et al., 2012). Together, these studies support the important physiological role of AQP3 in H_2O_2 permeation towards intracellular downstream signaling events, like differentiation and growing, migration and immune system function.

Likewise, AQP8 was also identified as an efficient H_2O_2 transporter (Bienert et al., 2007). Bertolotti and co-workers used a HeLa cell model expressing a fluorescent H_2O_2 sensor, Hyper, and an AQP inhibitor, mercurial compound. They observed that in presence of mercurial compound, the fluorescence signal decreased after the application of extracellular H_2O_2, indicating the AQP-mediated H_2O_2 uptake. In addition, they silenced the AQP8 expression in their cell model, and observed the same effect, the decrease of fluorescence signal when exposed cells to external H_2O_2, suggesting the AQP8 can promote H_2O_2 uptake (Bertolotti et al., 2013).

In contrast, AQP1 has been reported as unable to permeate H_2O_2 (Bienert et al., 2007; Miller et al., 2010). Experiments performed in HEK 293 cells showed not significant AQP1 contribution to H_2O_2 transport, since the diffusion of H_2O_2 across membranes was not affected when AQP1 was inhibited (Miller et al., 2010). Interestingly, a recent study suggested evidences that a physiological role of rat AQP1 as able to permeate H_2O_2 in rat aortic smooth muscle cells (rASMCs). They hypothesized that rAQP1 could be the cellular entry of H_2O_2 in rASMCs, while the AQP3 or AQP8 were not expressed in this cells. The siRNAs against AQP1 and a fluorescent H_2O_2 sensor Hyper were used to investigate the role of AQP1 in H_2O_2 permeation. As a result, it was observed a significant increase of intracellular fluorescence signal, when the cells were exposed to H_2O_2 external. However, in cells silenced with AQP1-siRNA, the H_2O_2 cellular entry was reduced. These evidences suggest a new physiological role of AQP1 in the transmembrane diffusion of H_2O_2 (Al Ghouleh et al., 2013).

1.2.3 Enzyme activities and H_2O_2 consumption

Even though H_2O_2 is able to diffuse across the cell membranes, when the cells are exposed to external H_2O_2, it is rapidly consumed inside the cell by antioxidant enzymes. However, this consumption is associated with the permeability characteristics of the cell membrane as a barrier to H_2O_2, which are dictated by its bilayer biophysical properties and by the presence of diffusion-facilitating channel proteins, such as AQPs (Bienert et al., 2007; Folmer et al., 2008). In mammalian cells the main H_2O_2-removing enzymes are catalase, glutathione peroxidase (GPx) and peroxiredoxins (Prx), whereas in *S. cerevisiae* cells, the cellular antioxidant enzymes mostly responsible to the catalysis of H_2O_2 are cytosolic catalase, cytochrome *c* peroxidase and glutathione peroxidase (Marinho, Cyrne, Cadenas, & Antunes, 2013), with peroxiredoxins relevance being still an open question. In mammalian cells, it is considered that the rate constant of H_2O_2 intracellular catabolism ($k_{catabolism}$) can be obtained by the sum of the rates constant of the reactions of H_2O_2 with different antioxidant enzymes: GPx (k_{GPx}), peroxiredoxins (k_{Prx}), and catalase ($k_{catalase}$), described as $k_{catabolism} = k_{GPx} + k_{Prx} + k_{catalase}$. The determination of GPx activity is a process more complex than catalase activity, and this is due to the fact that GPx is involved in a reaction mechanism with an oxidation-reduction cycle dependent of glutathione (GSH) as reducing agent. As GPx, the peroxiredoxins also need a reducing agent, thioredoxin, to restore their activity after reducing H_2O_2. In contrast, the decomposition of H_2O_2 by catalase is a simple dismutation reaction resulting water and oxygen, in which reducing agents are not needed (Eq. 1):

$$2\ H_2O_2 \xrightarrow{catalase} O_2 + 2\ H_2O \qquad (1)$$

For that reason the catalase activity can be easily measured *in situ* in permeabilized cells, since overall H_2O_2 consumption in cells with disrupted plasma membrane is only dependent on catalase if cells are incubated in a phosphate buffer (Marinho et al., 2013).

In yeast cells the H_2O_2 consumption is largely imposed by cytosolic catalase and mitochondrial cytochorome *c* peroxidase. Nevertheless, as with GPx, cytochrome *c* peroxidase requires the presence of its reduced substrate to complete its catalytic cycle. Thus, the disruption of yeast cells membrane in order to achieve the cytochrome *c* peroxidase activity is not as useful as for catalase, since the activity is limited in permeabilized cells due the absence of reduced substrates (Marinho et al., 2013).

1.3 AIMS AND GOALS

AQPs are a family of transmembrane proteins, which have been revealed as having an important role in disease progression such as some types of cancers. The involvement of AQPs in disease may be due to their physiology as channel and/or due to the effect of their transported molecules on other cellular processes associated with health and disease conditions such as oxidative stress. The role of AQPs involvement in disease due to their capacity to permeate H_2O_2 ought to be investigated.

Recently our group optimized a cell model for characterizing aquaporin activity and screening modulators using the yeast *Saccharomyces cerevisiae*. This heterologous expression system can be used to assess mammalian aquaporin function by the stopped-flow fluorescence technique, and was already validated for several aquaporin isoforms in respect to their selectivity to water and/or glycerol. Taking advantage of this yeast cell model, the role of the different AQPs in H_2O_2 permeation can be determined and correlated with their involvement in diseases.

Thus, this project aims to investigate the role of different AQPs in H_2O_2 permeation using the yeast *Saccharomyces cerevisiae* expression system previously developed in our group. For that, some mammalian-AQPs (AQP1, AQP3, AQP4, AQP5, AQP7 and AQP11) genes were cloned in an expression vector and used to transform *S. cerevisiae* strains. Strains were grown in the presence of different H_2O_2 concentrations to determine their sensitivity to H_2O_2 in a first approach. Finally, the H_2O_2 consumption of each AQP-transformed strain was measured with a hydrogen peroxide electrode, and the kinetic parameters were determined for the evaluation of membrane H_2O_2 permeation through the different mammalian-AQPs.

In summary, the specific goals were outlined as follow:

1. A first evaluation of the H_2O_2 sensitivity of the different strains through a drop test experiment, which is a screening of all strains expressing different mammalian-AQPs in presence of different H_2O_2 concentrations;
2. Optimization of the cell growth conditions in a new medium for subsequent H_2O_2 consumption measurements with the hydrogen peroxide electrode;
3. Quantification of mammalian-AQPs expression in the different strains using the fluorescence technique and measuring the cell membrane fluorescence intensity in order to assess the different expression levels;
4. Measurement of H_2O_2 consumption in the different strains using a hydrogen peroxide electrode and establishment of H_2O_2 kinetic parameters;

5. Finally, determination of catalase activity (an antioxidant enzyme) using the hydrogen peroxide electrode to measure the H_2O_2 consumption in permeabilized cells.

2. Materials and Methods

2.1 CELL LINES

The yeast cell model used for the experimental studies in this work was previously established by our group. Transformed yeast *Saccharomyces cerevisiae* strains were obtained in order to assess the permeability of water, glycerol and H_2O_2 through several AQPs. All the strains were transformed from the parental *Saccharomyces cerevisiae* YSH 1770, which is endogenous aquaporin-defective (AQY1 and AQY2 knock-out), and thus, deficient for glycerol and/or water transport. The different mammalian-AQPs gene sequences were previously cloned in an expression vector pUG35 (*Vector shuttle S. cerevisiae-E. coli, Amp^r, URA3*). This expression vector allows the cloning of any gene in line with the reporter gene yEGFP (*yeast-enhanced Green Fluorescence Protein*) thereby enabling the cellular localization of the expressed protein yEGFP fused. Lastly, the yeast strains were transformed by electroporation in selective conditions. All the strains and plasmids used in this work are described in Table 2.1.

Table 2.1. Description of the strains/plasmids used in this work and their references and characteristics.

Strains/Plasmids	Genotype/Relevant characteristics
YSH 1770	Double mutant strain aqy1 aqy2 (MATα leu2::hisG tpr1::hisG his3::hisG ura352 apy1D::KanMX aqy2D::KanMX)
YSH 1770/pUG35	YSH 1770 transformed with empty expression vector pUG35
YSH 1770/pUG35-AQP1	YSH 1770 transformed with gene *Rathus norvegicus AQP1* cloned in pUG35
YSH 1770/pUG35-AQP3	YSH 1770 transformed with gene *Rathus norvegicus AQP3* cloned in pUG35
YSH 1770/pUG35-AQP4	YSH 1770 transformed with gene M_1 *Rathus norvegicus* AQP4 cloned in pUG35
YSH 1770/pUG35-AQP5	YSH 1770 transformed with gene *Rathus norvegicus AQP5* cloned in pUG35
YSH 1770/pUG35-AQP7	YSH 1770 transformed with gene *Homo sapiens AQP7* cloned in pUG35
YSH 1770/pUG35-AQP11	YSH 1770 transformed with gene *Homo sapiens AQP11* cloned in pUG35

2.2 CELL CULTURE

All the culture media used for cells growth were sterilized after their preparation using an autoclave (*JP Selecta* and/or *AJC Uniclave 88*) during 20 minutes, with a temperature of 120ºC and 1 atm. The media compositions are detailed in annex (Annex 6.1).

The *S. cerevisiae* strains were kept on a plate or angled test tubes containing solid media YNB with 2% (w/v) glucose, 2% (w/v) of agar and complemented with aminoacids required for growth (tryptophan, histidine and leucine) at -8ºC. A new fresh streaking plate/test tube of each strain was made every month. For the drop test experiments, S. c*erevisiae* transformants were cultured in liquid YNB medium (identical to maintenance medium, without agar) at 28ºC with orbital shaking (180 rpm). For the experiments to quantity the cell membrane intensity by fluorescence microscopy and for the measurements of H_2O_2 consumption and catalase activity using a H_2O_2 electrode, the different strains were grown in SC (synthetic complete) medium without uracil, at 30ºC orbital shaking (180 rpm). Cell growth was monitored by measurement of the optical density at 600 nm (OD_{600}) using a spectrophotometer (*Ultrospec 2100 Pro* and/or *Thermo Scientific Genesys 10S*).

2.3 DROP TEST EXPERIMENT – A YEAST-BASED PHENOTYPIC ASSAY

The drop test experiment was chosen as a first assessment of H_2O_2 sensibility of strains expressing AQPs, and it was performed according to (Sabir et al., 2014). This method consists in a serial dilution of yeast cells strains and in comparing the cell growth rate of different strains under different H_2O_2 concentrations.

The drop test was performed on agar plates containing growth medium YNB (pH 5.0) with 2% (w/v) glucose and aminoacids required (tryptophan, histidine and leucine). Agar plates were prepared with six different H_2O_2 concentrations in duplicate (0.25, 0.5, 0.75, 1, 1.5 and 2 mM) and control plates (without H_2O_2 addition). These medium plates were prepared in the dark and at the same day that drop tests will be completed, to avoid H_2O_2 degradation by light. Yeast strains were previously grown overnight until $OD_{600nm} \approx 1$ (approximately 2-3 x 10^7 cells/ml) in liquid YNB medium 2% (w/v) glucose with tryptophan, histidine and leucine, at 28ºC with orbital shaking (180 rpm). Due to the different doubling time of the strains, the cells did not reach OD=1 at the same time. In order to ensure that the same number of cells of each AQP-transformed strains will be tested, the volumes were corrected according to the required cells number. For that, the strain with the lowest OD_{600nm} number was considered as the reference strain, with OD of reference, as well as the volume of culture was considered as volume of reference. Next, the

required number of cells was obtained and the volumes necessary of each strain were calculated according:

$$OD_{reference} \times 3 \times 10^7 = Amount\ Required\ (cell/ml)$$

$$Volume_{reference} \times Amount\ Required\ = Required\ cells\ number$$

$$\frac{Required\ Cells\ number}{OD_{strain} \times 3 \times 10^7} = Volume\ of\ strain$$

After the volumes of all the other strains were adjusted, cells were centrifuged and the resulting pellet was re-suspended in sterile distilled water in a multi-well plate. The multi-well plate was completed with a serial 10-fold dilutions of the original cells concentrated. A 3µL aliquot from each dilution was spotted using replica platter device into agar plates containing YNB solid medium, which were previously prepared with the different H_2O_2 concentrations. The *S. cerevisiae* strain transformed with empty vector (pUG35) was used as a control. Finally, the plates were incubated at 28°C and the results of growth and survival were recorded after 1 and 2 weeks of incubation. Figure 2.1 shows a schematic illustration of the drop test experimental procedure.

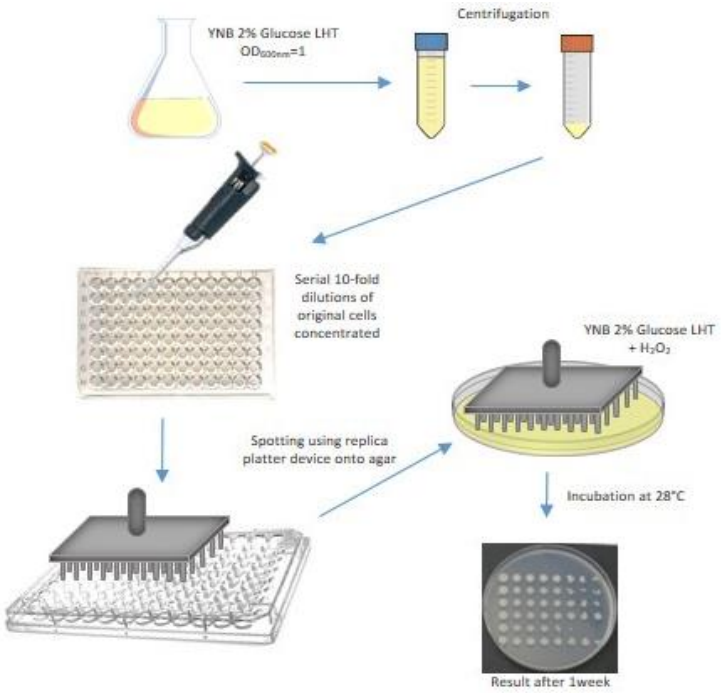

Figure 2.1. The drop test experimental procedure: AQP-transformed strains grew until OD_{600nm}=1, in liquid YNB medium with 2% glucose and tryptophan, histidine and leucine. Cells were centrifuged and the pellet was re-suspended in sterile distilled water in a multi-well plate. Serial 10-fold dilutions of the pellet of each AQP-transformed strains were prepared. Then, the spotting was implemented using replica platter device onto agar plates containing the different H_2O_2 concentrations. Finally, the plates were incubated at 28°C.

2.4 FLUORESCENCE METHOD

As aforesaid, the heterologous expression of mammalian-AQPs on yeast *Saccharomyces cerevisiae* strain used for experimental studies in this work was previously established by our group and validated for water and glycerol transport studies. These functional studies were performed in YNB medium with 2% (w/v) glucose supplemented with aminoacids required for growth (tryptophan, histidine and leucine). The detection of cellular location of the expressed AQPs with yGFP fused was already confirmed. However, in this work another growth media was used, the SC medium (described above in Methods). Therefore, the *S. cerevisiae* transformants strains, cultured in a new media (SC medium), were analyzed by fluorescence microscopy in order to validate the membrane localization of yGFP-tagged AQPs, as well as to assess AQPs expression levels. Thereby, cells were grown overnight in SC medium (without uracil) at 30ºC until reaching OD_{600nm}≈1. Then, a cell suspension aliquot was placed on a lamella subsequently assembled on an inverted fluorescence microscope (Zeiss Axiovert 200) equipped with a digital camera (CoolSNAP EZ, Photometrics, USA). For the cells observation, it was applied a lens 100x with immersion oil over 1.6x of microscope and the excitation wavelength of 495 nm. The fluorescence images were obtained with 120 seconds exposure time. The software used to the image acquisition was Metafluor and the AQPs expression levels were subsequently analyzed using ImageJ software (*http://imagej.nih.gov/ij/*).

2.4.1 Quantitative Analysis

The images obtained from the digital camera assembled in the fluorescence microscope were analyzed in order to validate the membrane localization, as well as to quantify the expression levels of the mammalian-AQPs in the different strains. As mentioned above, the expression vector pUG35, which was used to transform the different *S. cerevisiae* strains, allows the expression of AQP-isoform fused with GFP. Thereby, the detection of the cellular localization of each AQP in the different strains was achieved by GFP-tagging under fluorescence microscopy.

The protein localization can be confirmed through observation of images, once the fluorescence signal is easily and clearly identified in the cell membrane. In contrast, for the quantitative analysis, such as quantification of protein expression levels, several image analysis programs are available and they are useful tools. The ImageJ software was used to extract quantitative data about AQP-expression levels, by the measurement of the intensity of the cell membrane.

The first step performed using the ImageJ software was to adjust important settings in order to make the image analysis easier. Taking into consideration that AQP-transformed strains show different signal intensities, the Brightness/Contrast was adjusted equally for all the strains, in order to achieve a correct comparison of AQP-expression between strains. It was deliberated the basic values of adjustment 135-350, which corresponds to automatic Brightness/Contrast considered for AQP3, one of the observed strains with stronger fluorescence signal. Using a "straight line" toll from the ImageJ toolbar, it was drawn a line that is perpendicular to the cell membrane of interest, which crosses the membrane. Once the segmented line tool is selected, the intensity profile along the path can be plotted with the "Plot profile" tool. A graph of intensities was obtained, wherein the highest intensity value corresponding to the membrane signal intensity (Joshi & Davidson, 2010). This procedure was repeated to record three membrane intensity values from a single cell, and at least 80 cells were accounted of each AQP-transformed strain. Figure 2.2 illustrates the applied procedure for the image analysis using ImageJ. The background value was estimated using the "Oval selection" tool from the ImageJ toolbar by delimitation of a region without cells. Then, the "Measure" tool allows the access to the "results window", which is a list with estimated parameters of the outlined region, including the mean value. Lastly, it was calculated the median value of the three intensity values estimated per cell, and the background value was deducted.

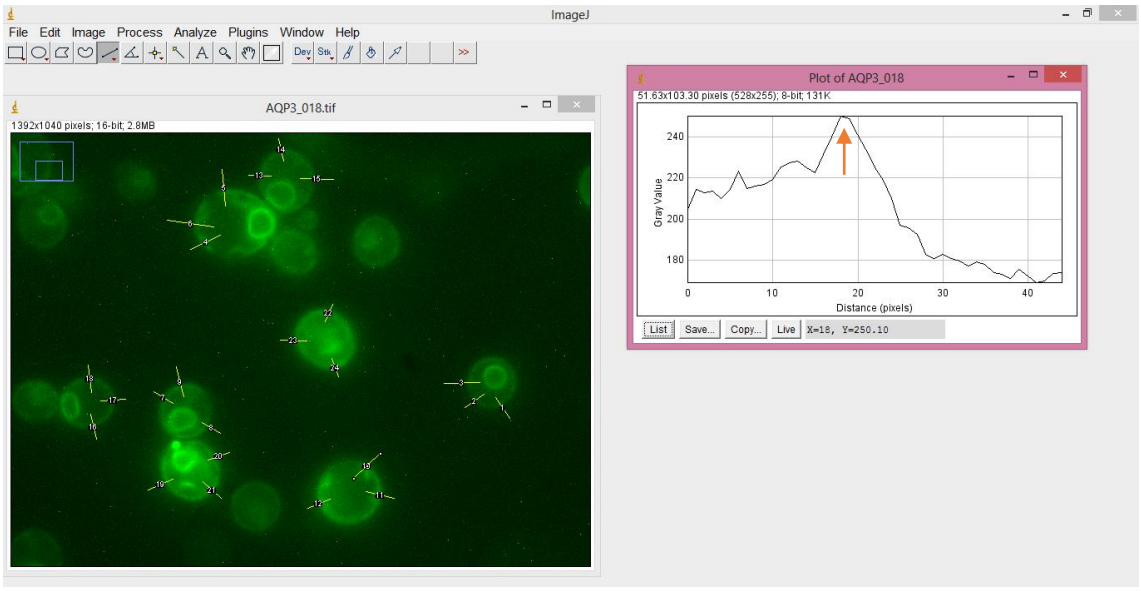

Figure 2.2. Demonstration of AQP3-expression analysis using ImageJ software. The first window (left side) shows a high resolution view of a fluorescence analyzed image of AQP3-transformed cells. The yellow numerated lines indicate the path of an intensity profile across a selected membrane using "straight line" tool. The second window (right side) represents a graph with the intensity profile along the path of a single line, which was obtained by "plot profile" command. The orange arrow indicates the highest value of intensity in the membrane of the selected line, corresponding to AQP3-expression level in the membrane of an AQP3-transformed cell (y=250.10).

2.5 DETERMINATION OF KINETICS OF THE H_2O_2 CONSUMPTION

In order to assess H_2O_2 permeation by the different AQPs, the H_2O_2 consumptions by the different AQP-transformed strains were determined by measurement of the actual H_2O_2 concentration present in the culture medium using a H_2O_2 electrode. The speed of the consumption of H_2O_2 inside the yeast cells does not solely depends on the capability to remove H_2O_2, i.e. the presence of H_2O_2-removing enzymes, but also depends on the membrane permeability to H_2O_2. On the other hand, the membrane permeability depends on the membrane properties as a barrier to H_2O_2, either by the free diffusion across membrane or by the presence of diffusion-facilitating channel proteins (Marinho et al., 2013). These experiments allowed achieving kinetics results about the H_2O_2 consumptions by the different AQP-transformed strains, which provided a real assessment of the role of different AQP-isoforms as a H_2O_2 diffusion-facilitating channel. The yeast strain transformed with the empty vector (pUG35) was used as a control, and the H_2O_2 consumptions measured in this yeast strain provided information about the H_2O_2 free diffusion across membrane.

2.5.1 Preparation of H_2O_2 solution

A stock solution with approximately 9mM was previously prepared by dilution 1/1000 of the concentrated H_2O_2 solution (Perhydrol 30% (m/m), density 1.11 g/mL, MW=34.02, 9.79 M, from Merck), which was carefully handled with gloves. While H_2O_2 solutions can be relatively unstable, the concentration of the stock solution needed to be standardized for accurate results of the H_2O_2 measurements. For that reason, the concentration was confirmed every week by reading the absorbance at 240 nm and using a molar extinction coefficient (ε) of 43.4 $M^{-1}cm^{-1}$ *(Marinho et al., 2013)*. The stock solution with a 9mM would have an A_{240nm} of approximately 0.390.

The H_2O_2 solution, which was used in H_2O_2 consumption assays, was made fresh every day from the stock solution of H_2O_2. So, in an *eppendorf* tube it was prepared a 1/10 dilution of H_2O_2 stock solution (100 µL + 900 µL of distilled water) and kept on ice without light.

2.5.2 Measurement of H_2O_2 consumption

As aforementioned, in order to assess the H_2O_2 consumption of each AQP-transformed strain, a hydrogen peroxide electrode was used to measure the actual H_2O_2 concentration present in the culture medium. The procedure was performed in a chamber with H_2O_2 electrode properly assembled with a magnetic stirrer and the circulating water bath thermostat (*ELMI Sky Line*) maintaining a controlled temperature (30°C). The electrode was linked to a free radical

analyzer system (*World Precision Instruments* TBR4100) directly connected to a PC for registration by the LabScribe software. The system detects the small current (pA) created by the oxidation of H_2O_2 on the surface of electrode. The current produced is linearly proportional to amount of H_2O_2 in the culture medium. The data acquisition software records the range of the voltage (in volt) per unit of time (in milliseconds), which are exported to subsequent data handling.

The electrode was polished every week and the permeable membrane was replaced every two-three days, depending on the quality of the recorded signal, and according the supplier instructions. After replacement of the permeable membrane, the system needs to stabilize the signal with the chamber filled with distilled water overnight. It is also important that the electrode shows a stable baseline before starting the assays. For this reason, it is necessary to add distilled water in the electrode chamber and to connect the stirring, as well as the external circulating bath thermostat, a few hours before the measurements.

The different AQP-transformed strains were previously grown in SC medium (without uracil) overnight at 30ºC until reaching OD_{600nm}≈1. Then, 3 mL culture of yeast cells was added to electrode chamber and the recording by the system started. After few minutes for the stabilization of the system, an aliquot of H_2O_2 solution already prepared (as described in 2.5.1) was added. The amount of H_2O_2 solution added (approximately 65-67 µL) depended on the concentration of the stock solution, which was checked and recalculated every week. Regardless, it was required that the final concentration of H_2O_2 inside the electrode chamber was 20 μM. This addition should cause a rapidly increase in the reading followed by a decrease of signal. The recording was carried out during the time required to obtain a constant decrease of signal, which allowed the kinetic parameters analysis. Finally, the content of the H_2O_2 electrode chamber was removed and in order to be sure that all the cells and H_2O_2 were removed before the following H_2O_2 consumption assay, the chamber was carefully cleaned a few times with distilled water.

The measurement of H_2O_2 consumption by the growth medium is also important. Since it was expected no consumption by SC medium, this experiment works as a control and provides information about media contaminations or about the operating system, such permeable membrane performance or the requirement to polish the electrode. Furthermore, the addition of medium in the H_2O_2 electrode chamber helps the electrode stabilization in the following experiments with yeast cells.

2.5.3 Data handling/Processing

As mentioned above, the current produced by the oxidation of H_2O_2 on the surface of electrode, was detected by the system and the data acquisition software recorded the range of the voltage (in volt) per unit of time (in milliseconds). Since the current produced is linearly proportional to the amount of H_2O_2 in the culture medium, it was possible to obtain the first-order rate constant (*k*) of H_2O_2 consumption by each AQP-transformed strain.

First, the baseline was deducted of the data recorded. The baseline is the constant voltage recorded once the cells were stabilized before the H_2O_2 addition. Then, the data obtained was plotted as logarithm of voltage versus time (ln(voltage) versus time). For a first-order decay, this plot is linear with a negative slope, i.e. the rate constant is determined from the slope (k=-slope), and has units $time^{-1}$. Lastly, it is necessary to take into account that the H_2O_2 will be consumed faster as the number of the yeast cells in the experiment. For that reason, the rate constant should be divided by the OD_{600} value to account for the accurate number of cells present (approximately OD_{600nm}=1). The software GraphPad Prism was used for the statistical analysis, with $P<0.05$ (marked as *) and $P<0.01$ (marked as **) considered to be statistically significant.

2.6 DETERMINATION OF CATALASE ACTIVITY

As already mentioned, the magnitude of H_2O_2 consumption not only depends on the presence of H_2O_2-removing enzymes, but also depends on the membrane permeability to H_2O_2, including the presence of diffusion-facilitating channel proteins, possibly the AQPs. Since the experiments were performed in altered yeast cells, which can lead to metabolic modifications, namely in proteins expression, it is necessary to investigate if the H_2O_2-removing enzymes expression is not affected in these strains. In yeast cells, the main H_2O_2-removing enzymes are cytosolic catalase along with cytochrome *c* peroxidase. However, the determination of the contribution of cytochrome *c* peroxidase to cellular H_2O_2 removal is more complex than that due to catalase.

In addition to the determination of H_2O_2 consumptions by the different strains, the activity of catalase was also determined in each AQP-transformed strain. This experiment aimed to assess if the catalase activity was not altered or increased in some AQP-transformed strains, and thus, to validate that the differences in the consumptions determined were only due the presence of AQPs.

Whereas the assays for the determination of H_2O_2 consumption were performed in intact cells, the experiments for the assessment of catalase activity *in situ* were determined in permeabilized yeast cells using the H_2O_2 electrode. In these experiments performed in permeabilized yeast cells, the overall H_2O_2 consumption rate is due to cytosolic catalase, which is the only active H_2O_2-removing enzyme under these experimental conditions. It is due to the fact that the other cellular antioxidants enzymes responsible to the catalysis of H_2O_2, such as cytochrome *c* peroxidase and GPx have limited activity because their reaction mechanism of catalysis involve reducing agents or substrates which are unavailable in permeabilized cells.

The determination of catalase activity was performed only in S. c*erevisiae* strains expressing AQP3-, AQP4- and AQP5-isoforms, as well as in the yeast strain transformed with the empty vector (pUG35), which was used as a control. The yeast AQP-transformed strains analyzed were chosen according to the results of the measurements of H_2O_2 consumption. Since the results suggested the AQP3-, AQP4- and AQP5-transformed strains as the major consumers of H_2O_2 (see below in Results and Discussion), and thus, as the best candidates for H_2O_2 channels, it was necessary to assess the catalase activity of these strains and to compare with the catalase activity of the control strain.

The permeabilization of yeast cells can be easily done using digitonin, which acts as a detergent and disrupts the plasma membrane. The commercial digitonin reagent (MW=1229, from Fluka) should not be used directly in experiments due the high impurities percentage (about 30-50%). In addition, the effects of unpurified digitonin are unpredictable and the impure material is not soluble in water. The purification was achieved by recrystallization, and the following procedure was carried out.

2.6.1 Digitonin Purification

The supplier recommended the purification method according to Kun et col. (Kun, Kirsten, & Piper, 1979). The method was performed with some modifications: 1g was dissolved in 25 ml of absolute ethanol at 75°C. Digitonin is precipitated by chilling the solution. However this chilling was preformed slowly in styrofoam box: first at room temperature, after that at -8°C and finally at -32°C. Then the solution was separated by centrifugation (2700 rpm during 4 minutes). The supernatant was removed and the procedure was repeated three times, resulting in approximately 60% (0.6 g) after drying at room temperature. The digitonin purified is soluble in water, yielding a clear apparent solution that become turbid after 1-2 hours standing. For this reason, the digitonin solution (10 mg/mL) was made fresh just before use.

2.6.2 Measurement of H_2O_2 consumption in permeabilized cells

The system used to measure the H_2O_2 consumption in intact yeast cells was reused to assess the catalase activity in the different AQP-transformed strains. In order to maintain the experimental conditions, all the experimental considerations and recommendations for the application of this method using the H_2O_2 electrode mentioned in 2.5.1 were taken into account. In addition, the preparation of H_2O_2 solution was performed every week as described in 2.5.2. The cells growth was performed in SC medium (without uracil) overnight at 30°C until reaching OD_{600nm}≈1. Subsequently, the electrode chamber was filled with 3 mL culture of yeast cells to analyze and the system started the recording. Then, an aliquot of 30 µL of the 10 mg/mL digitonin solution previously prepared was added. After incubation under stirring and temperature controlled (30°C) during 5 minutes, which is considered time enough for full permeabilization of the yeast cells, the H_2O_2 was added. As in previous assays using the H_2O_2 electrode, the final H_2O_2 concentration required in the electrode chamber was 20 μM, and therefore, the aliquot of H_2O_2 solution added (about 65-67 µL) depending on the concentration of the stock solution, which was checked and recalculated every week. The actual concentration of H_2O_2 was measured during the time required to obtain a constant decrease of signal. As in the previous assays, the yeast strains transformed with empty vector (pUG35) was used as a

control. Lastly, the content of the H_2O_2 electrode chamber was removed and the chamber was carefully washed a few times with distilled water in order to be sure that all the cells, H_2O_2 and digitonin were removed before the following H_2O_2 consumption assay.

2.6.3 Data handling/Processing

The data processing was similar to the described above (in 2.5.3) for the rate constant determination of the H_2O_2 consumption by the each AQP-transformed strains. As above explained, in permeabilized yeast cells, the overall H_2O_2 consumption rate is due to cytosolic catalase, which is the only active H_2O_2-removing enzyme under these experimental conditions. Thus, the activity of catalase ($k_{catalase}$) is obtained through the slope of the plot of ln(voltage) versus time.

3. Results

3.1 OPTIMIZATION OF THE CELL GROWTH CONDITIONS

The yeast *S. cerevisiae* expression system used in this work was previously established by our group and validated to water and glycerol transport studies. These functional studies were performed in YNB medium with 2% (w/v) glucose supplemented with aminoacids required for growth (tryptophan, histidine and leucine). In this work, the same growth medium was used for the sensibility study of different *S. cerevisiae* strains to H_2O_2. However, for the experiments using the hydrogen peroxide electrode such as the measurements of H_2O_2 consumption and catalase activity, a different culture medium was required (unpublished data). It was necessary to cultivate the *S. cerevisiae* strains expressing AQPs in SC medium to subsequent functional studies.

For this purpose, some growth curves were established. The growth rate defines the number of doublings that occur per unit of time, and stipulates the doubling time through the following equation:

$$Doubling\ time = \frac{\ln(2)}{Growth\ rate}$$

Figure 3.1. shows a growth curve of the yeast strain expressing mammalian-AQP1 and the respective exponential trendline equation.

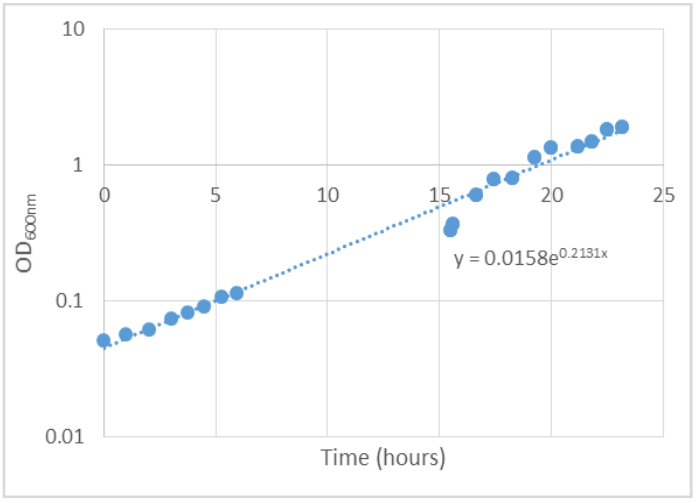

Figure 3.1. Illustration of a cell growth curve of AQP1-transformed strain when cultured in SC medium whit an OD_{600nm} value of 0.05. The fit to the exponential growth obtained shows a slope of 0.2131, stipulating the growth rate and consequently the doubling time of 3.25 hours for the yeast strain expressing AQP1.

In table 3.1 the resulting doubling time obtained for each transformed yeast strain cultured in SC medium without uracil are represented. From the results, we can observed that the doubling time of the different AQP-transformed strains differ greatly. In brief, the strain expressing AQP11 shows the slowest growth and close to reach 4 hours of doubling time (about 3.9 hours). In contrast, the AQP3 and AQP7-transformed strains had the fastest growth, around 3 hours of doubling time (about 3.1 hours), followed by AQP5 expressing strain with a doubling time of 3.2. Finally, the control strain pUG35 (transformed with empty vector), the strain expressing AQP1 and AQP4 showed a doubling time of 3.4, 3.3 and 3.5, respectively.

Table 3.1. The resulting doubling time (in hours) of each *S. cerevisiae* strains expressing different AQP-isoforms, as well as, the strain transformed with empty vector pUG35 cultured in SC media.

Yeast strain	**pUG35**	**AQP1**	**AQP3**	**AQP4**	**AQP5**	**AQP7**	**AQP11**
Doubling time (hours)	3.4	3.3	3.1	3.5	3.2	3.1	3.9

As expected, all the strains exceeded a doubling time of 3 hours, which allowed to realize that yeast doubling times were different than the previously doubling time determined in YNB media for our group (unpublished data). The SC medium has more constituents than YNB medium, which can lead to changes in yeast cell metabolism. These modifications can affect the proteins expression required to cell growth or to other important cellular processes. These data allow to conclude that the SC medium constituents influence the yeast strains growth.

3.2 SENSITIVITY OF THE DIFFERENT STRAINS TO H_2O_2

The drop test experiment allows the rapid analysis and a simple comparative evaluation of the H_2O_2 effect in cell growth of all strains expressing different mammalian-AQPs in the presence of different H_2O_2 concentrations. Additionally, this assay can indirectly identify some AQP as candidates for the transport of H_2O_2 across plasma membranes. In brief, the high concentrations of H_2O_2 can lead to metabolic disorders in an unidentified manner, which may induce reduction or impaired growth of yeast cells. Thus, an eventual increase of H_2O_2 permeability by some AQP-isoform might cause growth inhibition or cell death due the increase H_2O_2 influx into yeast cells.

Figure 3.2. shows the results of growth and survival of different AQP-transformed strains recorded after 1 week of incubation. In general, it was observed an impaired growth in all yeast strains at higher H_2O_2 concentrations. However, some yeast strains expressing some AQP isoforms demonstrate higher sensitivity to H_2O_2 than others. The strains expressing AQP1, AQP5 and AQP11 revealed some degree of inhibition for the first (and lower, 0.25mM) H_2O_2 concentration tested. Cells expressing AQP5 were the most inhibited, similar to AQP11 and followed by AQP1 and AQP3. Strains expressing AQP4 and AQP7 were the less affected by H_2O_2, and the strain expressing AQP7 showed similar growth as the control strain pUG35.

The growth sensitivity can indicate a putative role of some AQP-isoform in H_2O_2 transport, since an increase in H_2O_2 level into yeast cells can lead to disruptions in cellular metabolism. The H_2O_2 is a ROS, and due their reactive nature, they are able to damage proteins, lipids and nucleic acids. In addition, they can initiate several signal pathways leading to oxidative stress. For this reason, this molecule play an important role in cellular processes associated with cell death and growth conditions. At present, there is only evidence about AQP1, AQP3 and AQP8 as H_2O_2 transporters (Bienert & Chaumont, 2014; Miller et al., 2010), therefore it was expected some osmosensitivity of strain expressing AQP3 to the externally applied H_2O_2. Interestingly, AQP3-expressing strain showed tolerance to H_2O_2 and was able to grow as the control strain pUG35, regardless the H_2O_2 concentration exposure. Furthermore, the orthodox AQP1 was already referred in the literature as a membrane protein able to facilitate the diffusion of H_2O_2 (Al Ghouleh et al., 2013; Almasalmeh et al., 2014) even though that some findings contradicted this fact (Bienert et al., 2007; Miller et al., 2010). Our data show that strain expressing AQP1 has impairment in growth, and thus points to AQP1 as possible H_2O_2 carrier. The results also show that AQP4 and AQP7 are the most resistant strains to external H_2O_2, and thus we can assume that these AQP isoforms do not permeate H_2O_2. Regarding AQ11, data show

that AQP11-strain has a slow growth comparing to pUG35, even in the in absence of H_2O_2. This fact was also previously observed in growth curves, where this strain showed the largest doubling time, about 3.9 hours. However, in presence of H_2O_2 AQP11-transformed strain also showed reduced growth suggesting AQP11 as possible H_2O_2 transporter. Thus, based on the results from drop test assay, we can consider AQP5 as the best candidate for H_2O_2 transport, since it was the isoform most sensitive to external H_2O_2, as shown in Figure 3.1., wherein the osmosensitivity of AQP5 expressing strains is revealed since the lowest H_2O_2 concentration (0.25 *mM)*.

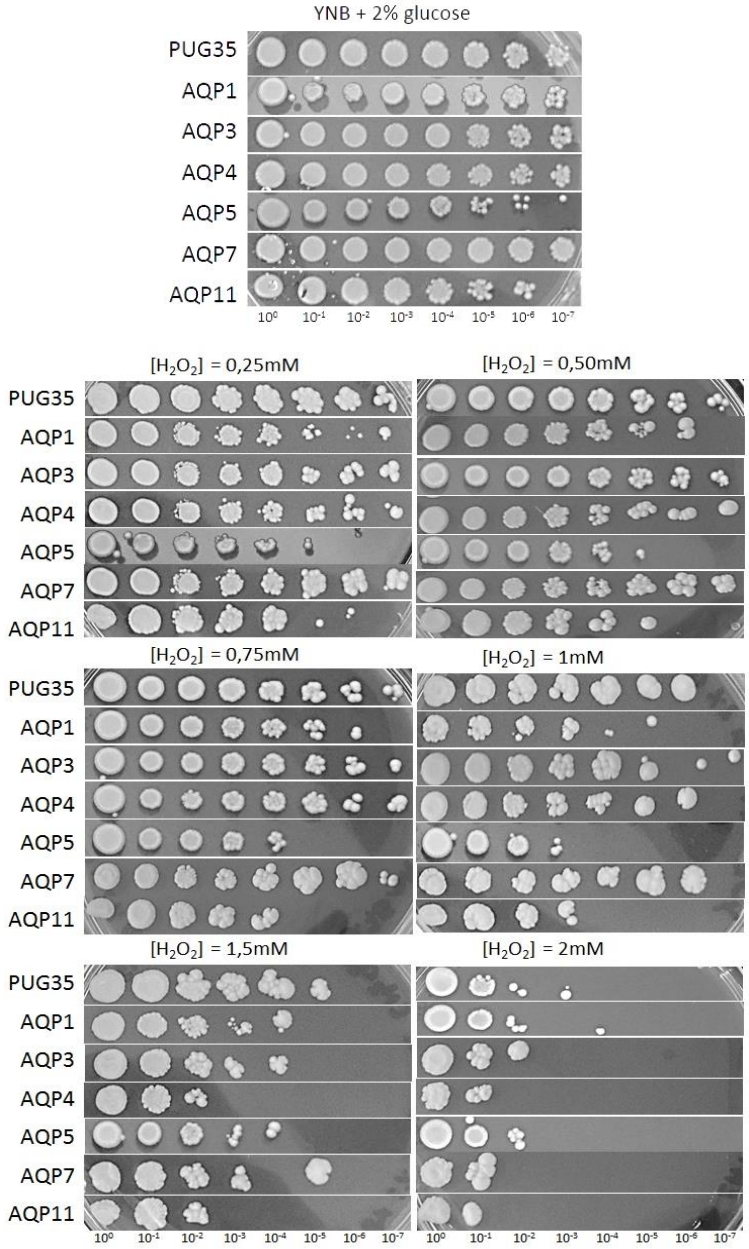

Figure 3.2. Growth assays of *S. cerevisiae* strains expressing different AQPs on solid YNB medium supplemented with 2% (w/v) glucose containing H_2O_2. Different yeast strains are spotted from the top to the bottom row in 10-fold dilution (from the left to the right column). The yeast strain with empty vector was the control (pUG35). Several H_2O_2 concentrations were tested (0.25mM to 2mM). These results were recorded after 1 week of incubation.

3.3 LOCALIZATION AND QUANTIFICATION OF MAMMALIAN-AQPS EXPRESSION

The expression and localization of the mammalian-AQPs cloned in yeast strains in SC media were investigated by GFP-tagging using the fluorescence microscopy method. In addition, this method was used to quantify the expression levels of these AQPs-isoforms.

Figure 3.3 shows the expression and localization of mammalian-AQPs expressed in *S. cerevisiae.* As depicted in figure, all the yeast strains transformed with AQP-isoforms, including the control cells transformed with empty plasmid pUG35, showed fluorescence, assuring that the GFP tag is being expressed. The cytosolic GFP accumulation in control cells is the result of GFP-free synthesis (none membrane protein GFP-fused) by cells transformed with the empty vector (figure 3.3 in A). In the AQP-transformed strains, the expression of GFP-tagged mammalian-AQPs was confirmed. The figures show that most of the GFP-tagged AQPs were localized in plasma membrane of the yeast cells, which suggest the correct intracellular trafficking of the synthesized AQPs to plasma membrane where they function as channels. Moreover, it was also observed that some of the GFP-tagged AQPs were retained inside the cell, perhaps in the endoplasmic reticulum or in vesicles of the secretory pathway. In contrast, the strain expressing AQP1 (figure 3.3 in B) shows the lowest fluorescence intensity and consequently, a lower expression level and a reduced amount of protein in membrane. Curiously, the fluorescent images of the strain expressing AQP1 show some similarities with the control cells, notably the cytosolic GFP-localization, suggesting that GFP-tagged AQP1 remained entrapped in the cell cytosol.

The mammalian-AQPs expression was quantified in order to correlate the expression levels with the H_2O_2 consumption by the different transformed strains. In table 3.2 it is shown the fluorescence intensity of the different strains accounted using the ImageJ software. As expected, the AQP1-transformed strain was the most difficult to evaluate due the reduced protein in membrane, and showed the lowest expression level. However, the strain expressing AQP5 and AQP7 also revealed low fluorescence intensity values. Additionally, we can observed that the yeast cells expressing AQP4 showed the highest florescence intensity, as observed in the image 3.3. (in D). Likewise, the AQP3-transformed strain shows a high expression level.

These expression levels related with the results of H_2O_2 consumption by different AQP-transformed strains are discussed below, considering that a promising AQP-isoform for H_2O_2 permeation should show a higher H_2O_2 consumption value when normalized by the abundance of AQP isoform in the strain studied.

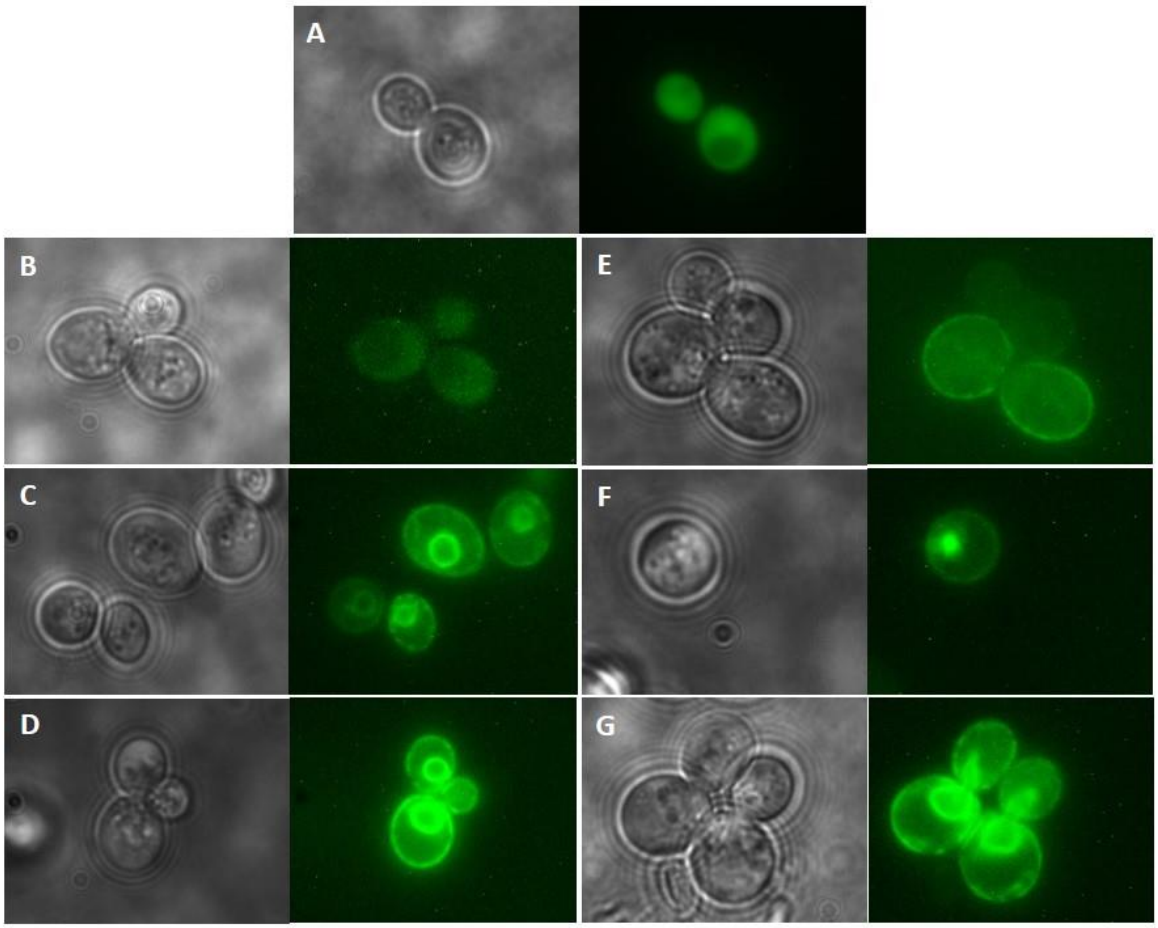

Figure 3.3. Expression and localization of GFP-tagged mammalian-aquaporins expressed in *S. cerevisiae* strains cultured in SC media. For each AQP-transformed strain, the image of visible-light is shown on the left panel, and the image taken by fluorescence microscopy is on the right panel. In *A*, the cytosolic yGFP-localization in cells transformed with empty plasmid pUG35 (control cells). The other images represent the membrane yGFP-localization in cells expressing AQP1 (B); AQP3 (C); AQP4 (D); AQP5 (E); AQP7 (F) and AQP11 (G).

Table 3.2. The fluorescence intensity quantified of each AQP-isoform expressed in *S. cerevisiae* strains cultured in SC media. Data are present as mean ± standard deviation (SD).

AQP-ISOFORM	FLUORESCENCE INTENSITY (N=80)
AQP1	**20.5** ± 8.5
AQP3	**72.1** ± 31
AQP4	**102.5** ± 43.5
AQP5	**25.7** ± 16.8
AQP7	**30.4** ± 11.5
AQP11	**49.7** ± 28.2

3.4 MEASUREMENT OF H_2O_2 CONSUMPTION

For the assessment of membrane H_2O_2 permeation through the different mammalian-AQPs, the H_2O_2 consumption of each AQP-transformed strain was analyzed. Thereby, the actual H_2O_2 concentration present in the culture medium was estimated, using a hydrogen peroxide electrode. As explain above (in Materials and Methods, 2.5.2), the system detects the small current created by the oxidation of H_2O_2 on the surface of electrode, and therefore the current produced is linearly proportional to amount of H_2O_2 in the culture medium. In the figure 3.4 is illustrated a typical signal recording of H_2O_2 consumption (in blue) using H_2O_2 electrode by *S. cerevisiae* strain transformed with empty vector pUG35, control cells (figure 3.4 in A) and *S. cerevisiae* strain transformed with AQP1-, AQP3-, AQP4-, AQP5-, AQP7- and AQP11-isoform (figure 3.4 in B, C, D, E, F and G, respectively). The software recorded the range of the voltage (in volt) per unit of time (in milliseconds). First, it can be observed a stabilization of signal when there were only yeast cells in electrode chamber. Then, an aliquot of H_2O_2 solution was added, leading an increase of signal. At that moment, the consumption by yeast cells started, so the signal tends to decrease. In order to establish a correct assessment H_2O_2 consumption by each transformed strain, it was required that all the strains were in the same OD_{600nm} value. In the same figure 3.4, in grey is represented the semi-logarithmic of voltage values versus time. The first-order kinetic rate constant (*k*) for the consumption of H_2O_2 by yeast cells was obtained from the slope of a plot of ln(voltage) versus time.

The control cells showed a first-order kinetic rate constant (*k*) for the consumption of H_2O_2 of $(1.5 \pm 0.2) \times 10^{-6}$ sec^{-1} collected from five independent experiments. The consumption by the control cells is due to free diffusion of H_2O_2 across yeast cell membranes, since there are no AQPs expressed in this yeast strain. Therefore, it was assumed that AQP-transformed strains with rate constant values higher than *k* calculated for the control cells, would have increased passive uptake of H_2O_2 due the AQPs-mediated transport.

As evident from the figure 3.4, the graphs seem similar to recording results of control cells (figure 3.4 in A), however they show different slopes of a plot of semi-logarithmic of voltage values. From six independent experiments, AQP1-transformed strain gave a first-order kinetic rate constant (*k*) for the consumption of H_2O_2 of $(1.8 \pm 0.2) \times 10^{-6}$ sec^{-1}, suggesting that this strain is more permeable to H_2O_2 than control strain (about 20%).

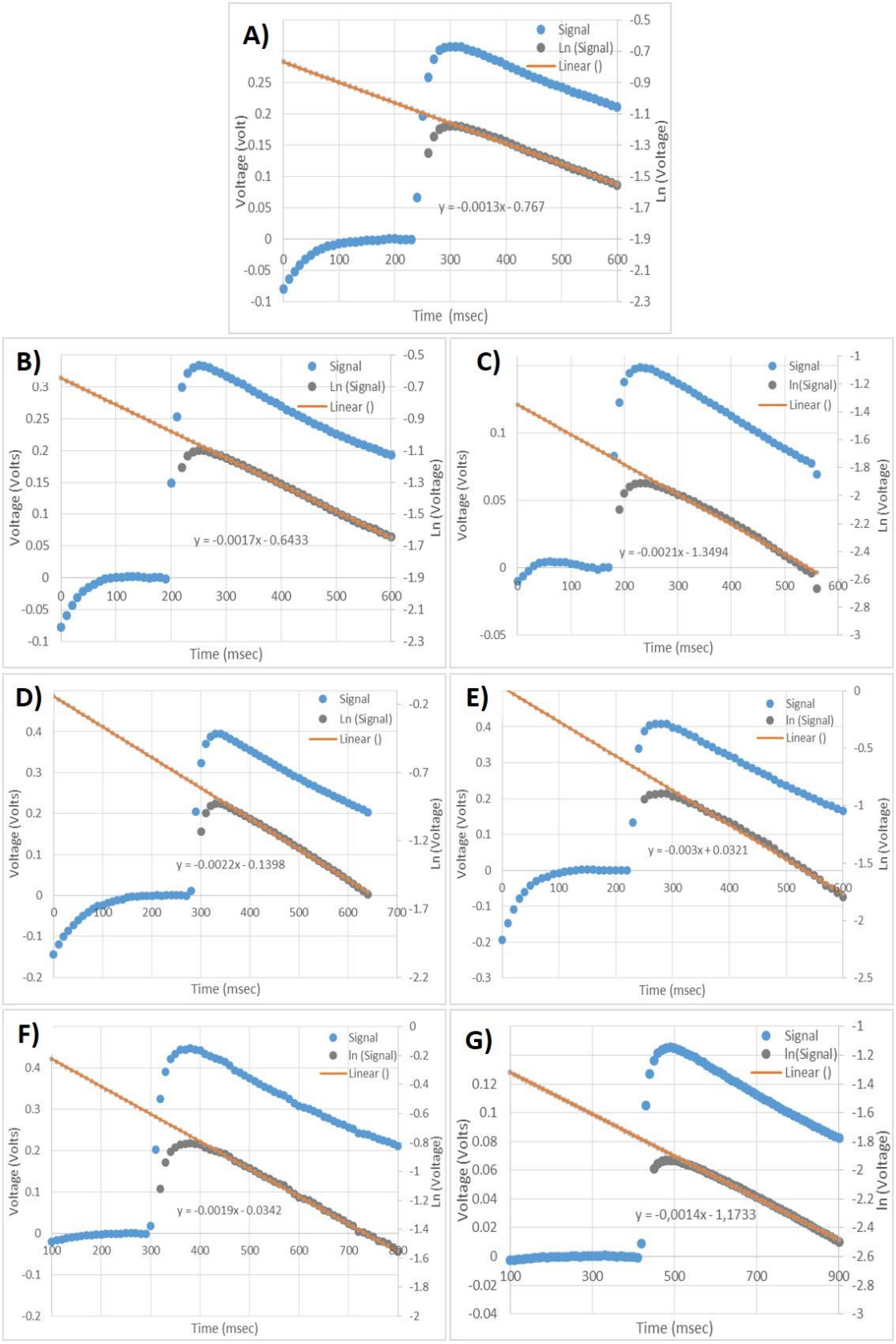

Figure 1.4. Exemplification of the determination of the rate constants in *S. cerevisiae* strain transformed with empty vector pUG35, i.e. the control cells (A) and *S. cerevisiae* strain transformed with AQP1-isoform (B), AQP3-isoform (C), AQP4-isoform (D), AQP5-isoform (E), AQP7-isoform (F) and AQP11-isoform (G). All the strains were cultured in SC media. In blue is exemplified the typical recording of a H_2O_2 consumption with the H_2O_2 electrode. In grey, it is represented the ln(Voltage) versus time (msec). The rate constant was obtained from the slope of a plot of ln(voltage) versus time.

The first-order kinetic rate constant (*k*) calculated for the consumption of H_2O_2 by AQP3-expresing strain was (2.2 ± 0.5) × 10^{-6} sec^{-1}, collected from five independent experiments. Considering the clear difference between *k* values of control strain and AQP3-expressing strain (approximately 40%), we can suppose that AQP3 isoform can be a promising H_2O_2 channel protein. In fact, AQP3 was already reported in the literature as a H_2O_2 channel.

AQP4-transformed strain gave a first-order kinetic rate constant (*k*) for the consumption of H_2O_2 of (2.3 ± 0.4) × 10^{-6} sec^{-1} collected from six independent experiments. The increase of about 50% of H_2O_2 consumption by yeast cells expressing AQP4 comparing with the control, provides evidence that AQP4 is a promising candidate to permeate H_2O_2.

The yeast cells expressing AQP5-isoform showed the most promising results, with a first-order kinetic rate constant (*k*) for the consumption of H_2O_2 of (2.4 ± 0.5) × 10^{-6} sec^{-1} collected from seven independent experiments. The satisfactory about 60% increase of H_2O_2 consumption when compared with control strain, suggests the putative role of AQP5 in the transmembrane diffusion of H_2O_2, and points to its role as a H_2O_2 channel.

The first-order kinetic rate constant (*k*) calculated for the consumption of H_2O_2 by AQP7-transformed strain was (1.9 ± 0.2) × 10^{-6} sec^{-1}, collected from five independent experiments. Lastly, the AQP11-expressing strain obtained a first-order kinetic rate constant (*k*) for the consumption of H_2O_2 of (1.9 ± 0.5) × 10^{-6} sec^{-1}, collected from five independent experiments.

Table 3.3 shows a summary of the H_2O_2 consumption results obtained for each AQP-transformed strain.

Table 3.3. First-order kinetic rate constant (*k*) of the H_2O_2 consumption obtained for each AQP-transformed strains cultured in SC media. All the strains were analyzed with OD_{600nm}=1. Data are present as mean ± standard deviation (SD).

	RATE CONSTANT (*k*) × 10^{-6} (sec^{-1})	**$k/k_{control}$**
PUG35	(**1.6** ± 0.1) (n=5)	1
AQP1	(**1.8** ± 0.2) (n=6)	1.2
AQP3	(**2.2** ± 0.5) (n=5)	1.4
AQP4	(**2.3** ± 0.4) (n=6)	1.5
AQP5	(**2.4** ± 0.5) (n=7)	1.6
AQP7	(**1.9** ± 0.2) (n=5)	1.2
AQP11	(**1.9** ± 0.5) (n=5)	1.2

Multiple comparisons test generated by the software GraphPad Prism was used for the statistical analysis. P<0.05 (marked as *) and P<0.01 (marked as **) were considered to be statistically significant and are identified in bar graph of figure 3.5. Even though all the strains show an increase of H_2O_2 permeability compared to control strain based on experimental assays, only the strains expressing AQP4 e AQP5 were considered to be statistically significant. However, the AQP3-expressing strain also showed satisfactory results, in fact, with a confidence level of 90%, with an adjusted P value of 0.0769.

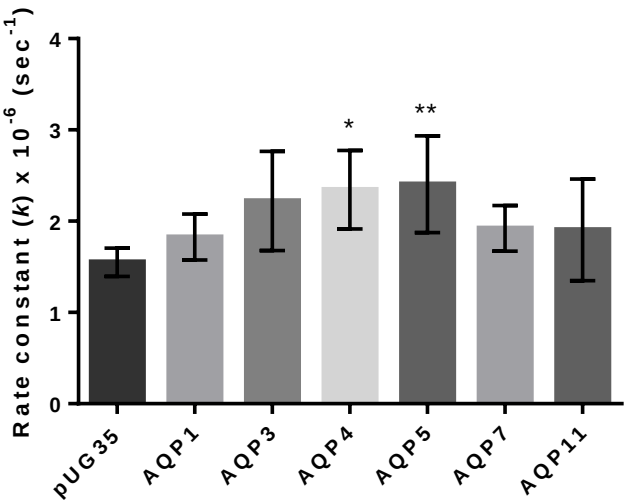

Figure 3.5. Graphical representation of first-order kinetic rate constant (*k*) of the H_2O_2 consumption obtained for each AQP-transformed strains cultured in SC media, as well as, *k* value obtained by control cells. Data are expressed as mean ± standard deviation (SD). Multiple comparisons test was used to statistical analysis. The comparisons between first-order kinetic rate constant (*k*) of the H_2O_2 consumption obtained by control cells ant the *k* value obtained for each AQP-transformed strains cultured in SC media. Family-wise significance and confidence levels (CI): P<0.05 (marked as *) and P<0.01 (marked as **) were considered to be statistically significant.

3.5 DETERMINATION OF CATALASE ACTIVITY

As already mentioned (in 2.6 of Materials and Methods), the magnitude of H_2O_2 consumption not only depends on the membrane permeability to H_2O_2, which includes the presence of diffusion-facilitating channel proteins, but also depends on the intracellular presence of H_2O_2-removing enzymes. Taking into account that the present study used a heterologous AQP-expression system in *S. cerevisiae* strains, the fact that these altered yeast cells can have metabolic changes, specifically in protein expression, cannot be ruled out. In this regard, the investigation of whether H_2O_2-removing enzymes expression is not affected in these strains is of particular interest. Given that a key H_2O_2-removing enzymes is cytosolic catalase, the catalase activity was determined in order to validate the results of H_2O_2 consumption by AQPs-transformed strains already investigated.

These experiments were performed only in the S. c*erevisiae* strains expressing AQP3-, AQP4- and AQP5-isoforms, which based in the experiments already carried out, were considered the best candidates for H_2O_2 permeation. Results were compared with the catalase activity measured in control cells, transformed with empty vector pUG35. In order to do so, it was needed the permeabilization of yeast cells, using digitonin, and the H_2O_2 electrode was used to measure the actual H_2O_2 concentration present in the culture media. In permeabilized yeast cells, the overall H_2O_2 consumption rate is due to cytosolic catalase, which is the only active H_2O_2-removing enzyme under these experimental conditions, because does not need reducing equivalents.

Figure 3.6 shows a typical recording results of H_2O_2 consumption by catalase (in blue) of the control permeabilized cells (figure 3.6 in A) and *S. cerevisiae* permeabilized cells transformed with AQP3-, AQP4- and AQP5-isoform (figure 3.6 in B, C and D, respectively). These graphs have similarities with the recording results previously performed to measure the H_2O_2 consumption by the intact cells of different AQP-transformed strains. First, the permeabilized cells in the chamber stabilized and an aliquot of H_2O_2 solution was added. At that moment there was a fast signal increase until 0.5V and then, the catalase in the permeabilized cells initiated the H_2O_2 decomposition, leading to a decrease of the signal. H_2O_2 will be decomposed to H_2O and O_2 as faster as the amount of the catalase. In order to establish a correct assessment of catalase activity, it was required that all the strains were in the same OD_{600} value. In figure 3.6, the semi-logarithmic of voltage values versus time is represented in orange. Catalase activity ($k_{catalase}$) in permeabilized cells was obtained from the slope of a plot of ln(voltage) versus time.

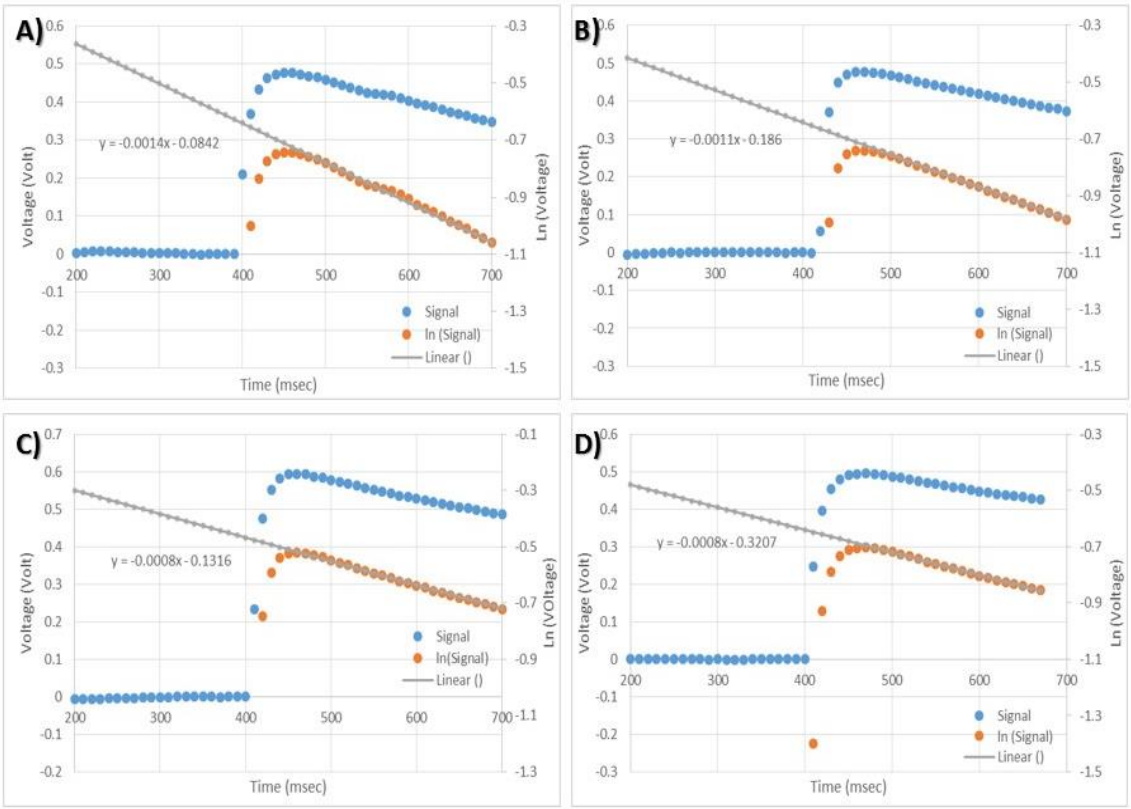

Figure 3.6. Exemplification of the determination of the $k_{catalase}$ in *S. cerevisiae* permeabilized cells transformed with empty vector pUG35, i.e. the control permeabilized cells (A) and *S. cerevisiae* permeabilized cells transformed with AQP3-isoform (B), AQP4-isoform (C) and AQP5-isoform (D). In blue are exemplified the typical recording of a H_2O_2 consumption by catalase. In orange it is represented the plot of ln(voltage) versus time (msec). The rate constant was obtained from the slope of a plot of ln(voltage) versus time.

Table 3.4 shows a summary of the catalase activity results obtained for each AQP-transformed strain analyzed, as well as the behavior compared to the control strain. The control cells gave a rate constant ($k_{catalase}$) for the catalase activity of (1.1 ± 0.2) x 10^{-6} sec^{-1} collected from four independent experiments. All the AQP-transformed strains analyzed showed a lower catalase activity than control strain, whereas the yeast strain transformed with AQP5-isoform showed the lowest $k_{catalase}$, (0.66 ± 0.06) x 10^{-6} sec^{-1} (n=4), with a decrease of about 40% comparing to the $k_{catalase}$ in control cells. The AQP3-expressing strains showed a $k_{catalase}$ of (0.8 ± 0.2) x 10^{-6} sec^{-1} collected from five independent experiments. Finally, the $k_{catalase}$ obtained for the permeabilized yeast cells expressing AQP4 was of (0.8 ± 0.2) x 10^{-6} sec^{-1} collected from four independent experiments.

Table 3.4. Rate constant ($k_{catalase}$) of H_2O_2 consumption by catalase obtained for permeabilized cells of AQP-transformed strains analyzed. All the strains were cultured in SC media and were analyzed with OD_{600nm}=1. Data are present as mean ± standard deviation (SD).

	RATE CONSTANT ($k_{catalase}$) × 10^{-6} (sec^{-1})	$k_{catalase}/k_{catalase\_control}$
PUG35	(**1.1** ± 0.2) (n=4)	1
AQP3	(**0.8** ± 0.2) (n=5)	1.3
AQP4	(**0.8** ± 0.2) (n=4)	1.3
AQP5	(**0.66** ± 0.06) (n=4)	1.4

This experiment aimed to investigate whether the catalase activity, a H_2O_2-removing enzyme, was not altered or increased in some AQP-transformed strains, and thus, to validate that the differences in the H_2O_2 consumptions by transformed strains determined in this present work were only due the presence of AQPs supporting their roles as H_2O_2 channels. Based on the results, we can suppose that catalase activity is altered but not increased in AQP-transformed strains, and consequently, the evidences for AQP3, AQP4 and AQP5 as H_2O_2 channels were not contradicted. Thus, the higher rate constants of H_2O_2 consumption by AQP-transformed strains were not due to altered catalase activity, but due to capacity of some AQPs-isoforms to H_2O_2 transport. However, this study provides further understanding on metabolic changes, specifically regarding protein expression in these strains. On one hand, the fact that the catalase activity is diminished in our transformed yeast cells, reinforce these AQP-isoforms as the best candidates as H_2O_2 channels. Nevertheless, it may be concluded that the AQPs heterologous expression caused metabolic changes on yeast cells, which should be considered and investigated in further studies.

4. Discussion

As mentioned above, our research group previously developed the heterologous expression model used in this work in order to assess the permeability of water and glycerol. In this project, the permeability of H_2O_2 of the different AQP-transformed strains was also evaluated. The water and glycerol permeation were analyzed by stopped-flow fluorescence technique, a method that allows the determination of physical parameters required to calculate membrane permeability, as well as the activation energy for transport. Briefly, the conclusions of the functional study are that the strain expressing AQP5 shows the highest osmotic water permeability coefficient (P_f), followed by AQP1 and AQP4-expressing strains (unpublished data). What is more, the presence of water-channels was confirmed by using a well-known inhibitor of aquaporin function (the mercurial reagent $HgCl_2$). All the AQP expressing strains demonstrated a clear decrease of P_f value in presence of the mercurial compound. In addition, the strains expressing AQP3 and AQP7 showed to permeate glycerol in addition to water. These data were important in the context of the present work, because they report that all the mammalian-AQPs are already functionally tested and are active water and/or glycerol channels.

In the present work, the first approach was a screening of growth sensitive test of all AQP-transformed strains in presence of different H_2O_2 concentrations in order to assess their role in H_2O_2 permeation. The reduced growth and survival showed by AQP5- and AQP11-transformed strains suggests their ability to transport H_2O_2.

After an optimization of cell growth conditions in a new media, the subcellular localization by GFP-tagging and fluorescence technique was confirmed. The results indicate that all GFP-tagged AQPs were localized in plasma membrane of the yeast cells although it was also observed some intracellular retention, perhaps in the endoplasmic reticulum or in vesicles of the secretory pathway. In addition, the mammalian-AQPs expression in the different strains was quantified using fluorescence microscopy in order to assess the different expression levels, and subsequent correlation with the respective results of H_2O_2 consumption. The AQP1- and AQP5-transformed strains showed the lowest expression level. While the strain expressing AQP3 and AQP4 revealed the highest fluorescence intensity, resulting in a high expression level.

The functional studies of H_2O_2 consumption by the different strains were implemented using a H_2O_2 electrode and the kinetic parameters were determined. We have analyzed six mammalian-AQPs, and have shown that three of them facilitate the H_2O_2 transport in yeast cells. AQP3-, AQP4- and AQP5-expressing strains showed rate constant values for the H_2O_2 consumption of $(2.2 \pm 0.5) \times 10^{-6}$ sec^{-1} (n=5), $(2.3 \pm 0.4) \times 10^{-6}$ sec^{-1} (n=6), and $(2.4 \pm 0.5) \times 10^{-6}$

sec^{-1} (n=7), respectively. Therefore, about 40%, 50% and 60% higher than rate constant value obtained for control cells.

The expression levels along with the results of H_2O_2 consumption by different AQP-transformed strains are shown in Figure 4.1. The values of consumption were normalized [(consumption$_{AQP}$ – consumption$_{control}$)/expression level] in order to evaluate the H_2O_2 transport for each expressed AQP. Figure 4.1 shows the AQP expression level quantified as the fluorescence signal intensity and the rate constant (*k*) calculated for the consumption of H_2O_2 for each AQP-isoform expressed in *S. cerevisiae* strains. The normalized H_2O_2 consumption is represented in figure 4.2.

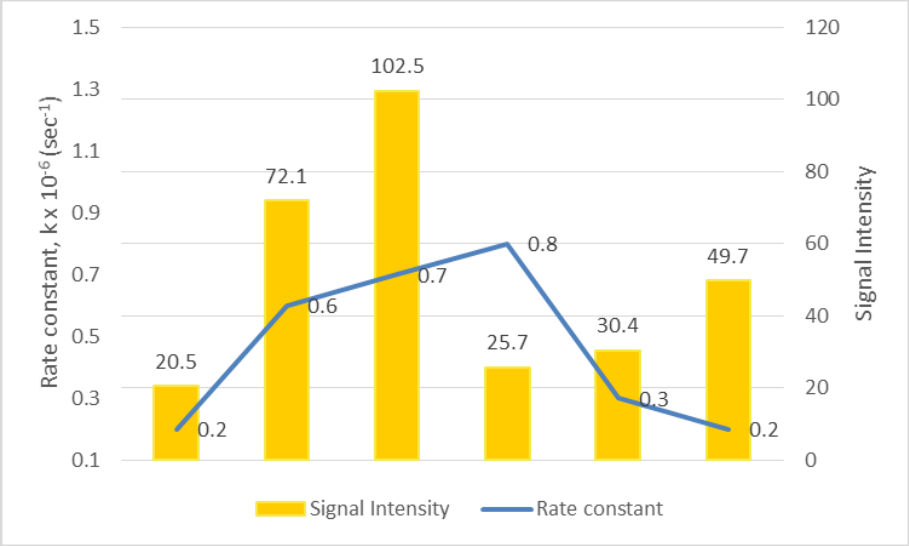

Figure 4.1. Correlation between the fluorescence signal intensity quantified and the rate constant (*k*) calculated for the consumption of H_2O_2 for each AQP-isoform expressed in *S. cerevisiae* strains cultured in SC media. In blue are represented the *k* values (in sec^{-1}) obtained for each AQP-isoform, with H_2O_2 free diffusion deducted (*k* value calculated for control strain). The yellow bars identify the fluorescence intensity of signal, classifying the AQP-expression level.

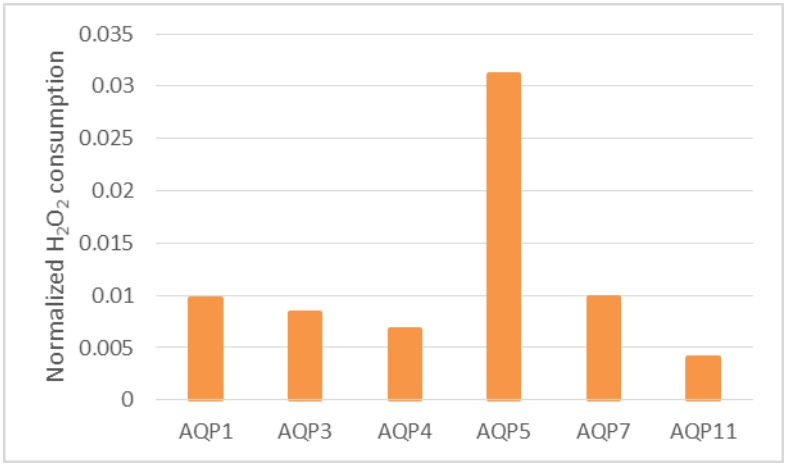

Figure 4.2. Normalized H_2O_2 consumption for each AQP-expressing strains. The normalization was achieved by using the equation: [(consumption$_{AQP}$ – consumption$_{control}$)/expression level].

Some contradicting findings on the H_2O_2 transport by AQP1 (Bienert et al., 2007; Miller et al., 2010), as well as, the physiological evidence for H_2O_2 permeability of AQP1 have been reported in some studies (Al Ghouleh et al., 2013; Almasalmeh et al., 2014). The drop test experiment revealed that the strain expressing AQP1 exhibits reduced growth in H_2O_2 presence, probably due the higher entrance of H_2O_2 through AQP. As evident from figure 4.1, strain expressing AQP1, which shows a low expression level, shows also a lower rate constant for the consumption of H_2O_2 comparing with others AQP-isoforms. In fact, the AQP1 was the most difficult AQP-isoform to quantify due its low expression. Thus, the low expression level can explain the poor H_2O_2 consumption by AQP1-expressing strain. Therefore, the results about AQP1 as a H_2O_2 transporter are still not clear.

The aquaglyceroporin AQP3 was already identified as a transmembrane protein able to diffuse H_2O_2 (Bienert et al., 2007; Miller et al., 2010). In fact, the AQP3-expressing strain gave a high *k* value, with an increase of about 40% of H_2O_2 consumption compared with the control strain. Indeed, this finding about AQP3 is in agreement with the previous reported when AQP3 was referred as a H_2O_2 channel. Nevertheless, the results of expression levels showed that AQP3-expressing strain was one of the strains showing the higher expression level. In fact, its high AQP-expressing level does not invalidate the capacity of AQP3 to permeate H_2O_2. Although, the high H_2O_2 consumption by AQP3-transformed strain can be explained by its high expression level, the putative role of AQP3 in permeation of H_2O_2 cannot be ruled out.

The drop test results showed that AQP4 is one of the more resistant strains to external H_2O_2. These data suggest that AQP4 is not able to facilitate H_2O_2 uptake. In contrast, the direct measurements of H_2O_2 transport performed reveal that AQP4-expressing strain has a high *k* value, with a difference about 50% of control cells. On the other hand, yeast cells expressing AQP4 showed the highest fluorescence intensity signal, as can be observed in figure 4.1. Thus, these data point to the high expression level of AQP4 in yeast cells responsible for the increased input molecules of H_2O_2 by this strain. Thus, by observing the rate constant value obtained we can conclude that AQP4 works as a H_2O_2 channel.

In the phenotypic assay performed in present study, the strain expressing AQP5 showed high sensitivity to external H_2O_2, being considered as the best candidate to H_2O_2 transport across cellular membrane. This promising evidence was confirmed in functional studies of H_2O_2 consumption using a H_2O_2 electrode, where AQP5-expressing cells gave the highest rate constant value for H_2O_2 consumption, about 60% higher than the *k* value obtained for yeast

control cells. Interestingly, the AQP5-transformed strain showed a low AQP5 expression level, (figure 4.1). As can be observed in figure 4.2, the higher normalized H_2O_2 consumption obtained by AQP5-transformed strain reinforces the role of this AQP-isoform in H_2O_2 permeation. Thus, in the present work, the role of AQP5 in permeate H_2O_2 was confirmed for the first time, suggesting its association with oxidative stress situations and all the pathologies where H_2O_2 is involved.

Yeast strain expressing the aquaglyceroporin-7 showed to be the most resistant AQP-transformed strain when exposed to external H_2O_2, which disqualified AQP7 as H_2O_2 carrier. Afterwards, the low rate constant value obtained reveal poor ability of AQP7 to H_2O_2 permeation. However, the strain expressing AQP7 also revealed low fluorescence intensity value. As similar to AQP1, we assume the role of AQP7 in H_2O_2 permeation across biomembranes as inconclusive, since the low H_2O_2 consumption by AQP7-expressing cells could be explained by the low AQP7 expression verified in transformed strain.

The AQP11 expressing strain showed the slowest growth and the drop test experiment performed revealed that AQP11 is a possible candidate for H_2O_2 permeation, due the sensitivity to external H_2O_2 observed. However, this evidence was promptly ruled out due the lowest *k* value for H_2O_2 consumption obtained among the different AQP-expressing yeast cells. In addition, the AQP11-transformed strain showed a relatively high expression of AQP11. Taken together, the data obtained in the present work indicate that AQP11 is unable to permeate H_2O_2 across plasma membrane.

Finally, the activity of catalase, an antioxidant enzyme responsible for the main H_2O_2 consumption, was determined in three AQP-transformed strains in order to investigate if the H_2O_2-removing enzyme expression is not altered or increased in these transformed strains. The results confirmed that catalase activity is not increased in AQP-transformed strains, validating that the differences in the H_2O_2 consumptions by transformed strains determined can be due the presence of AQPs, and therefore, supporting their putative role in H_2O_2 transport.

5. Conclusions

AQPs are a family of transmembrane proteins that have been reported as being more than simple water channels and having physiologically importance for cellular processes in living organisms, including tumor progression. Their involvement of AQPs in tumor growth may be due to the physiology of AQPs as channel and/or due to the effect of their transported molecules on other cellular processes associated with health and disease conditions. Evidence from studies reveal that specific AQP-isoforms, including AQP3, facilitate the passive diffusion of H_2O_2 across biomembranes, the most abundant reactive oxygen specie (ROS) in the organism, which has for long been correlated with tumor development. Such physiological evidence for H_2O_2 permeability of some AQPs and the association of ROS with several pathological conditions, such as oxidative stress triggered by H_2O_2 and their involvement in carcinogenesis initiation, motivated us to assess the role of AQPs in H_2O_2 transport. For this purpose, a yeast *Saccharomyces cerevisiae* expression system previously developed by our group was used for the functional analysis of six mammalian AQP-isoforms.

In summary, the results suggested AQP3 and AQP4 as having the capability to permeate H_2O_2. However, the combined tests of growth sensitivity assays in presence of H_2O_2, determination of H_2O_2 consumption in AQP5-transformed strains, and the quantification of AQP5-expression level in transformed strains provided evidence for the AQP5-isoform as a putative channel for H_2O_2. Therefore, it was established the relation of AQP5 with many functions having H_2O_2 as intervenient, including oxidative stress. Furthermore, AQP5 has been reported as associated in development of several cancer types, having increased expression in tumoral tissues. Given these evidences, the capability of AQP5 to permeate H_2O_2 and its association with tumor progression should be further investigated. In conclusion, the modulation/inhibition of AQPs expression and function may be a novel target for therapeutic approaches for cancer treatment.

Further studies are required to explore the role of AQPs in H_2O_2 transport. The results of this study could be clarified by using other methods to measure the H_2O_2 transport such as using a fluorescent H_2O_2 sensor, Hyper. The expression and/or activity of H_2O_2-removing enzymes, namely cytochrome *c* peroxidase, could also be evaluated in these transformed yeast strains. In addition, the H_2O_2 permeation by AQPs should be confirmed using for mammalian cell lines. Taking advantage of the available heterologous expression system, the role of others AQP-isoforms in H_2O_2 transport can be analyzed, such as the aquaglyceroporin-9. Finally, the role of AQPs in mediating fluxes of others unexpected solutes with physiological significance can also be explored.

6. References

Agre, P., Saboori, A. M., Asimos, A., & Smith, B. L. (1987). Purification and partial characterization of the Mr 30,000 integral membrane protein associated with the erythrocyte Rh(D) antigen. *J Biol Chem, 262*(36), 17497-17503.

Al Ghouleh, I., Frazziano, G., Rodriguez, A. I., Csanyi, G., Maniar, S., St Croix, C. M., . . . Pagano, P. J. (2013). Aquaporin 1, Nox1, and Ask1 mediate oxidant-induced smooth muscle cell hypertrophy. *Cardiovasc Res, 97*(1), 134-142. doi: 10.1093/cvr/cvs295

Almasalmeh, A., Krenc, D., Wu, B., & Beitz, E. (2014). Structural determinants of the hydrogen peroxide permeability of aquaporins. *FEBS J, 281*(3), 647-656. doi: 10.1111/febs.12653

Antunes, F., & Cadenas, E. (2000). Estimation of H2O2 gradients across biomembranes. *FEBS Lett, 475*(2), 121-126.

Benga, G. (2003). Birth of water channel proteins-the aquaporins. *Cell Biol Int, 27*(9), 701-709.

Bertolotti, M., Bestetti, S., Garcia-Manteiga, J. M., Medrano-Fernandez, I., Dal Mas, A., Malosio, M. L., & Sitia, R. (2013). Tyrosine kinase signal modulation: a matter of H2O2 membrane permeability? *Antioxid Redox Signal, 19*(13), 1447-1451. doi: 10.1089/ars.2013.5330

Bienert, G. P., & Chaumont, F. (2014). Aquaporin-facilitated transmembrane diffusion of hydrogen peroxide. *Biochim Biophys Acta, 1840*(5), 1596-1604. doi: 10.1016/j.bbagen.2013.09.017

Bienert, G. P., Moller, A. L., Kristiansen, K. A., Schulz, A., Moller, I. M., Schjoerring, J. K., & Jahn, T. P. (2007). Specific aquaporins facilitate the diffusion of hydrogen peroxide across membranes. *J Biol Chem, 282*(2), 1183-1192. doi: 10.1074/jbc.M603761200

Bienert, G. P., Schjoerring, J. K., & Jahn, T. P. (2006). Membrane transport of hydrogen peroxide. *Biochim Biophys Acta, 1758*(8), 994-1003. doi: 10.1016/j.bbamem.2006.02.015

Carbrey, J. M., & Agre, P. (2009). Discovery of the aquaporins and development of the field. *Handb Exp Pharmacol*(190), 3-28. doi: 10.1007/978-3-540-79885-9_1

Chae, Y. K., Kang, S. K., Kim, M. S., Woo, J., Lee, J., Chang, S., . . . Moon, C. (2008). Human AQP5 plays a role in the progression of chronic myelogenous leukemia (CML). *PLoS One, 3*(7), e2594. doi: 10.1371/journal.pone.0002594

Dynowski, M., Schaaf, G., Loque, D., Moran, O., & Ludewig, U. (2008). Plant plasma membrane water channels conduct the signalling molecule H2O2. *Biochem J, 414*(1), 53-61. doi: 10.1042/BJ20080287

Folmer, V., Pedroso, N., Matias, A. C., Lopes, S. C., Antunes, F., Cyrne, L., & Marinho, H. S. (2008). H2O2 induces rapid biophysical and permeability changes in the plasma membrane of Saccharomyces cerevisiae. *Biochim Biophys Acta, 1778*(4), 1141-1147. doi: 10.1016/j.bbamem.2007.12.008

Fruehauf, J. P., & Meyskens, F. L., Jr. (2007). Reactive oxygen species: a breath of life or death? *Clin Cancer Res, 13*(3), 789-794. doi: 10.1158/1078-0432.CCR-06-2082

Fruehauf, J. P., & Trapp, V. (2008). Reactive oxygen species: an Achilles' heel of melanoma? *Expert Rev Anticancer Ther, 8*(11), 1751-1757. doi: 10.1586/14737140.8.11.1751

Gorin, M. B., Yancey, S. B., Cline, J., Revel, J. P., & Horwitz, J. (1984). The major intrinsic protein (MIP) of the bovine lens fiber membrane: characterization and structure based on cDNA cloning. *Cell, 39*(1), 49-59.

Hachez, C., & Chaumont, F. (2010). Aquaporins: a family of highly regulated multifunctional channels. *Adv Exp Med Biol, 679*, 1-17.

Haddoub, R., Rutzler, M., Robin, A., & Flitsch, S. L. (2009). Design, synthesis and assaying of potential aquaporin inhibitors. *Handb Exp Pharmacol*(190), 385-402. doi: 10.1007/978-3-540-79885-9_19

Hara-Chikuma, M., Chikuma, S., Sugiyama, Y., Kabashima, K., Verkman, A. S., Inoue, S., & Miyachi, Y. (2012). Chemokine-dependent T cell migration requires aquaporin-3-mediated hydrogen peroxide uptake. *J Exp Med, 209*(10), 1743-1752. doi: 10.1084/jem.20112398

Hara-Chikuma, M., & Verkman, A. S. (2008). Prevention of skin tumorigenesis and impairment of epidermal cell proliferation by targeted aquaporin-3 gene disruption. *Mol Cell Biol, 28*(1), 326-332. doi: 10.1128/MCB.01482-07

Henzler, T., & Steudle, E. (2000). Transport and metabolic degradation of hydrogen peroxide in Chara corallina: model calculations and measurements with the pressure probe suggest transport of H(2)O(2) across water channels. *J Exp Bot, 51*(353), 2053-2066.

Ishibashi, K. (2009). New members of mammalian aquaporins: AQP10-AQP12. *Handb Exp Pharmacol*(190), 251-262. doi: 10.1007/978-3-540-79885-9_13

Ishibashi, K., Hara, S., & Kondo, S. (2009). Aquaporin water channels in mammals. *Clin Exp Nephrol, 13*(2), 107-117. doi: 10.1007/s10157-008-0118-6

Ishibashi, K., Kondo, S., Hara, S., & Morishita, Y. (2011). The evolutionary aspects of aquaporin family. *Am J Physiol Regul Integr Comp Physiol, 300*(3), R566-576. doi: 10.1152/ajpregu.90464.2008

Jablonski, E. M., Mattocks, M. A., Sokolov, E., Koniaris, L. G., Hughes, F. M., Jr., Fausto, N., . . . McKillop, I. H. (2007). Decreased aquaporin expression leads to increased resistance to apoptosis in hepatocellular carcinoma. *Cancer Lett, 250*(1), 36-46. doi: 10.1016/j.canlet.2006.09.013

Joshi, S. D., & Davidson, L. A. (2010). Live-cell imaging and quantitative analysis of embryonic epithelial cells in Xenopus laevis. *J Vis Exp*(39). doi: 10.3791/1949

Kafe, H., Verbavatz, J. M., Cochand-Priollet, B., Castagnet, P., & Vieillefond, A. (2004). Collecting duct carcinoma: an entity to be redefined? *Virchows Arch, 445*(6), 637-640. doi: 10.1007/s00428-004-1124-z

Kun, E., Kirsten, E., & Piper, W. N. (1979). Stabilization of mitochondrial functions with digitonin. *Methods Enzymol, 55*, 115-118.

Li, J., Wang, Z., Chong, T., Chen, H., Li, H., Li, G., . . . Li, Y. (2014). Over-expression of a poor prognostic marker in prostate cancer: AQP5 promotes cells growth and local invasion. *World J Surg Oncol, 12*(1), 284. doi: 10.1186/1477-7819-12-284

Lin, M. T., & Beal, M. F. (2006). Mitochondrial dysfunction and oxidative stress in neurodegenerative diseases. *Nature, 443*(7113), 787-795. doi: 10.1038/nature05292

Lippert, A. R., Van de Bittner, G. C., & Chang, C. J. (2011). Boronate oxidation as a bioorthogonal reaction approach for studying the chemistry of hydrogen peroxide in living systems. *Acc Chem Res, 44*(9), 793-804. doi: 10.1021/ar200126t

Liu, S., Zhang, S., Jiang, H., Yang, Y., & Jiang, Y. (2013). Co-expression of AQP3 and AQP5 in esophageal squamous cell carcinoma correlates with aggressive tumor progression and poor prognosis. *Med Oncol, 30*(3), 636. doi: 10.1007/s12032-013-0636-2

Liu, Y. L., Matsuzaki, T., Nakazawa, T., Murata, S., Nakamura, N., Kondo, T., . . . Katoh, R. (2007). Expression of aquaporin 3 (AQP3) in normal and neoplastic lung tissues. *Hum Pathol, 38*(1), 171-178. doi: 10.1016/j.humpath.2006.07.015

Liu, Z., Shen, J., Carbrey, J. M., Mukhopadhyay, R., Agre, P., & Rosen, B. P. (2002). Arsenite transport by mammalian aquaglyceroporins AQP7 and AQP9. *Proc Natl Acad Sci U S A, 99*(9), 6053-6058. doi: 10.1073/pnas.092131899

Macey, R. I., & Farmer, R. E. (1970). Inhibition of water and solute permeability in human red cells. *Biochim Biophys Acta, 211*(1), 104-106.

Machida, Y., Ueda, Y., Shimasaki, M., Sato, K., Sagawa, M., Katsuda, S., & Sakuma, T. (2011). Relationship of aquaporin 1, 3, and 5 expression in lung cancer cells to cellular differentiation, invasive growth, and metastasis potential. *Hum Pathol, 42*(5), 669-678. doi: 10.1016/j.humpath.2010.07.022

Madeira, A., Fernandez-Veledo, S., Camps, M., Zorzano, A., Moura, T. F., Ceperuelo-Mallafre, V., . . . Soveral, G. (2014). Human aquaporin-11 is a water and glycerol channel and localizes in the vicinity of lipid droplets in human adipocytes. *Obesity (Silver Spring), 22*(9), 2010-2017. doi: 10.1002/oby.20792

Maeda, N., Funahashi, T., & Shimomura, I. (2008). Metabolic impact of adipose and hepatic glycerol channels aquaporin 7 and aquaporin 9. *Nat Clin Pract Endocrinol Metab, 4*(11), 627-634. doi: 10.1038/ncpendmet0980

Mager, W. H., & Winderickx, J. (2005). Yeast as a model for medical and medicinal research. *Trends Pharmacol Sci, 26*(5), 265-273. doi: 10.1016/j.tips.2005.03.004

Manning, B. D., & Cantley, L. C. (2007). AKT/PKB signaling: navigating downstream. *Cell, 129*(7), 1261-1274. doi: 10.1016/j.cell.2007.06.009

Marinho, H. S., Cyrne, L., Cadenas, E., & Antunes, F. (2013). The cellular steady-state of H2O2: latency concepts and gradients. *Methods Enzymol, 527*, 3-19. doi: 10.1016/B978-0-12-405882-8.00001-5

Miller, E. W., Dickinson, B. C., & Chang, C. J. (2010). Aquaporin-3 mediates hydrogen peroxide uptake to regulate downstream intracellular signaling. *Proc Natl Acad Sci U S A, 107*(36), 15681-15686. doi: 10.1073/pnas.1005776107

Mitsuoka, K., Murata, K., Walz, T., Hirai, T., Agre, P., Heymann, J. B., . . . Fujiyoshi, Y. (1999). The structure of aquaporin-1 at 4.5-A resolution reveals short alpha-helices in the center of the monomer. *J Struct Biol, 128*(1), 34-43. doi: 10.1006/jsbi.1999.4177

Moon, C., Soria, J. C., Jang, S. J., Lee, J., Obaidul Hoque, M., Sibony, M., . . . Mao, L. (2003). Involvement of aquaporins in colorectal carcinogenesis. *Oncogene, 22*(43), 6699-6703. doi: 10.1038/sj.onc.1206762

Moura, T. F. (2004). Cristalografia e Função de Canais Membranares. *Revista da Sociedade de Química,* 27-37.

Nico, B., & Ribatti, D. (2010). Aquaporins in tumor growth and angiogenesis. *Cancer Lett, 294*(2), 135-138. doi: 10.1016/j.canlet.2010.02.005

Pop-Busui, R., Sima, A., & Stevens, M. (2006). Diabetic neuropathy and oxidative stress. *Diabetes Metab Res Rev, 22*(4), 257-273. doi: 10.1002/dmrr.625

Preston, G. M., & Agre, P. (1991). Isolation of the cDNA for erythrocyte integral membrane protein of 28 kilodaltons: member of an ancient channel family. *Proc Natl Acad Sci U S A, 88*(24), 11110-11114.

Preston, G. M., Carroll, T. P., Guggino, W. B., & Agre, P. (1992). Appearance of water channels in Xenopus oocytes expressing red cell CHIP28 protein. *Science, 256*(5055), 385-387.

Sabir, F., Leandro, M. J., Martins, A. P., Loureiro-Dias, M. C., Moura, T. F., Soveral, G., & Prista, C. (2014). Exploring Three PIPs and Three TIPs of Grapevine for Transport of Water and Atypical Substrates through Heterologous Expression in aqy-null Yeast. *PLoS One, 9*(8), e102087. doi: 10.1371/journal.pone.0102087

Shan, T., Cui, X., Li, W., Lin, W., & Li, Y. (2014). AQP5: a novel biomarker that predicts poor clinical outcome in colorectal cancer. *Oncol Rep, 32*(4), 1564-1570. doi: 10.3892/or.2014.3377

Shi, Z., Zhang, T., Luo, L., Zhao, H., Cheng, J., Xiang, J., & Zhao, C. (2012). Aquaporins in human breast cancer: identification and involvement in carcinogenesis of breast cancer. *J Surg Oncol, 106*(3), 267-272. doi: 10.1002/jso.22155

Sidel, V. W., & Solomon, A. K. (1957). Entrance of water into human red cells under an osmotic pressure gradient. *J Gen Physiol, 41*(2), 243-257.

Smith, B. L., & Agre, P. (1991). Erythrocyte Mr 28,000 transmembrane protein exists as a multisubunit oligomer similar to channel proteins. *J Biol Chem, 266*(10), 6407-6415.

Soveral, G. T., Moura, T. F. (2011). Aquaporin water channels. *Canal BQ- Revista da Sociedade Portuguesa de Bioquímica,* 36-43.

Valko, M., Rhodes, C. J., Moncol, J., Izakovic, M., & Mazur, M. (2006). Free radicals, metals and antioxidants in oxidative stress-induced cancer. *Chem Biol Interact, 160*(1), 1-40. doi: 10.1016/j.cbi.2005.12.009

Verkman, A. S. (2008). Mammalian aquaporins: diverse physiological roles and potential clinical significance. *Expert Rev Mol Med, 10*, e13. doi: 10.1017/S1462399408000690

Verkman, A. S. (2009). Knock-out models reveal new aquaporin functions. *Handb Exp Pharmacol*(190), 359-381. doi: 10.1007/978-3-540-79885-9_18

Verkman, A. S. (2011). Aquaporins at a glance. *J Cell Sci, 124*(Pt 13), 2107-2112. doi: 10.1242/jcs.079467

Verkman, A. S., Anderson, M. O., & Papadopoulos, M. C. (2014). Aquaporins: important but elusive drug targets. *Nat Rev Drug Discov, 13*(4), 259-277. doi: 10.1038/nrd4226

Verkman, A. S., Hara-Chikuma, M., & Papadopoulos, M. C. (2008). Aquaporins--new players in cancer biology. *J Mol Med (Berl), 86*(5), 523-529. doi: 10.1007/s00109-008-0303-9

Wittmann, C., Chockley, P., Singh, S. K., Pase, L., Lieschke, G. J., & Grabher, C. (2012). Hydrogen peroxide in inflammation: messenger, guide, and assassin. *Adv Hematol, 2012*, 541471. doi: 10.1155/2012/541471

Woo, J., Lee, J., Chae, Y. K., Kim, M. S., Baek, J. H., Park, J. C., . . . Moon, C. (2008). Overexpression of AQP5, a putative oncogene, promotes cell growth and transformation. *Cancer Lett, 264*(1), 54-62. doi: 10.1016/j.canlet.2008.01.029

Yang, J., Yan, C., Zheng, W., & Chen, X. (2012). Proliferation inhibition of cisplatin and aquaporin 5 expression in human ovarian cancer cell CAOV3. *Arch Gynecol Obstet, 285*(1), 239-245. doi: 10.1007/s00404-011-1908-8

Zeidel, M. L., Ambudkar, S. V., Smith, B. L., & Agre, P. (1992). Reconstitution of functional water channels in liposomes containing purified red cell CHIP28 protein. *Biochemistry, 31*(33), 7436-7440.

Zhang, Z., Chen, Z., Song, Y., Zhang, P., Hu, J., & Bai, C. (2010). Expression of aquaporin 5 increases proliferation and metastasis potential of lung cancer. *J Pathol, 221*(2), 210-220. doi: 10.1002/path.2702

7. Annexes

6.1 MEDIA COMPOSITIONS

- **Composition of YNB culture media**

Compound	Final Concentration
Yeast Nitrogen Base	0,67% (w/v)
Glucose	2% (w/v)
Histidine	20 mg/ml
Leucine	40 mg/ml
Tryptophan	30 mg/ml
Agar*	2% (w/v)

*For a solid YNB media.

- **Composition of SC (Synthetic Complete) culture media**

Compound	Final Concentration (**w**/v)
Yeast Nitrogen Base	0.685%
Glucose	2%
Histidine	0.01%
Leucine	0.01%
Tryptophan	0.005%
Adenine	0.0025%
Serine	0.04%
Threonine	0.02%
SC mix:	
- Arginine	0.002%
- Methionine	0.002%
- Tyrosine	0.003%
- Isoleucine	0.003%
- Lysine	0.003%
- Phenylalanine	0.005%
- Glutamic Acid	0.01%
- Valine	0.015%
- Aspartic Acid	0.01%

Note: All the media compounds must be sterile. It was made a stock solution of each compound of SC media. In preparation of some aminoacids it was necessary the addition of NaOH (10 mM) to facilitate the dissolution.